Available online at www.sciencedirect.com

ScienceDirect

journal homepage: www.elsevier.com/locate/he

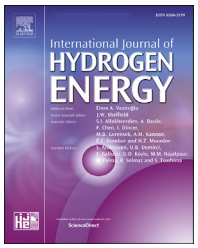

Simulating offshore hydrogen production via PEM electrolysis using real power production data from a 2.3 MW floating offshore wind turbine

Torbjørn Egeland-Eriksen [a,b,c,*], *Jonas Flatgård Jensen* [a], *Øystein Ulleberg* [d], *Sabrina Sartori* [a]

[a] *Department of Technology Systems, University of Oslo, Gunnar Randers Vei 19, 2007, Kjeller, Norway*
[b] *NORCE Norwegian Research Centre AS, Sørhauggata 128, 5527, Haugesund, Norway*
[c] *UNITECH Energy Research and Development Center AS, Spannavegen 152, 5535, Haugesund, Norway*
[d] *Institute for Energy Technology, Instituttveien 18, 2007, Kjeller, Norway*

HIGHLIGHTS

- Simulations of H_2 produced with electricity from real-world offshore wind turbine.
- Novel combination of electrolyzer model + wind power and electricity price data.
- H_2 production and cost vary by a factor of three between different periods.
- Highest H_2 production in a 31-day period was 17 242 kg with a 1.852 MW electrolyzer.
- The lowest H_2 production cost achieved was 4.53 $/kg H_2.

ARTICLE INFO

Article history:
Received 7 February 2023
Received in revised form
27 March 2023
Accepted 31 March 2023
Available online 26 April 2023

Keywords:
Offshore wind power
Hydrogen production
PEM electrolysis

ABSTRACT

This work presents simulation results from a system where offshore wind power is used to produce hydrogen via electrolysis. Real-world data from a 2.3 MW floating offshore wind turbine and electricity price data from Nord Pool were used as input to a novel electrolyzer model. Data from five 31-day periods were combined with six system designs, and hydrogen production, system efficiency, and production cost were estimated. A comparison of the overall system performance shows that the hydrogen production and cost can vary by up to a factor of three between the cases. This illustrates the uncertainty related to the hydrogen production and profitability of these systems. The highest hydrogen production achieved in a 31-day period was 17 242 kg using a 1.852 MW electrolyzer (i.e., utilization factor of approximately 68%), the lowest hydrogen production cost was 4.53 $/kg H_2, and the system efficiency was in the range 56.1–56.9% in all cases.

* *Corresponding author*. Department of Technology Systems, University of Oslo, Gunnar Randers Vei 19, 2007, Kjeller, Norway.
E-mail address: torbjorn.egeland-eriksen@its.uio.no (T. Egeland-Eriksen).

https://doi.org/10.1016/j.ijhydene.2023.03.471

Nomenclature:

Abbreviations

BoP	Balance of Plant
CAPEX	Capital Expenditure
FOWT	Floating Offshore Wind Turbine
HHV	Higher Heating Value
LCOH	Levelized Cost Of Hydrogen
LCOS	Levelized Cost Of Storage
LHV	Lower Heating Value
Li-ion	Lithium ion
OCV	Open-Circuit Voltage
OPEX	Operating Expenses
PEM	Proton Exchange Membrane
PV	Photovoltaic
SOC	State of Charge
SOFC	Solid Oxide Fuel Cell
SOEL	Solid Oxide Electrolyzer

Chemical elements

C	Carbon
H	Hydrogen
Li	Lithium
O	Oxygen

Non-SI units and conversion to SI

bar, unit of pressure 1 bar = 100 000 Pa
h (hour), unit of time 1 h = 3600 s
kWh (kilowatthour), unit of energy 1 kW h = 3 600 000 J
liter, unit of volume 1 L = 0.001 m^3
minute, unit of time 1 min = 60 s
year, unit of time 1 year = 31 536 000 s

Multiples used with SI units

Kilo (k) 10^3
Mega (M) 10^6
Giga (G) 10^9

Currencies

€	Euro, currency in the European Union
$	US dollar, currency in the United States of America
£	British pound, currency in the United Kingdom
CNY	Chinese yuan, currency in China
NOK	Norwegian krone, currency in Norway
AUD	Australian dollar, currency in Australia

Introduction

Climate change and geopolitical issues are key drivers for a faster transition from the use of fossil fuels to the use of renewable energy-based fuels and technologies. There is also an increased focus on the use of hydrogen as an energy carrier. If hydrogen is produced via water electrolysis with power from renewable energy (i.e., "green hydrogen") and used to reduce fossil fuels, global emissions of greenhouse gases could be significantly reduced. Possible applications include the use of hydrogen as an energy storage in electricity systems (both grid-connected and off-grid systems), hydrogen for the transport sector (both in fuel cells and combustion engines), use of hydrogen in industrial processes (e.g., production of ammonia, steel, and cement), or simply the use of hydrogen as a fuel for heating and cooking (as replacement for or mixed with natural gas).

A specific opportunity that has emerged in recent years is the combination of offshore wind power and hydrogen production via water electrolysis. Several pilot projects that will demonstrate this concept are in the planning phase: TechnipFMC will test a pilot system onshore during the next two years in their *Deep Purple*-project [1] and intend to use the results from this in a subsequent full-scale offshore system; Siemens Gamesa and Siemens Energy are cooperating on the development of a full-scale offshore wind turbine with integrated water electrolysis that they plan to demonstrate by 2026 [2]; Neptune Energy is planning to convert an oil platform into a platform that combines wind power and hydrogen production in their *PosHYdon*-pilot project [3]; ERM Dolphyn is in an early stage of development of a large-scale solution for hydrogen production from offshore wind and is aiming for the first commercial offshore hydrogen wind farm in the mid-to-late 2020's and the first GW-scale farm in the early 2030's [4].

The main objective of the work presented in this paper was to simulate and study the operation of a wind/hydrogen system based on a floating offshore wind turbine (FOWT) and hydrogen production via water electrolysis. A semi-empirical proton exchange membrane (PEM) water electrolyzer system model developed in MATLAB/Simulink in a previous project was used as basis for the technical modeling, while data from an existing 2.3 MW FOWT that has been in operation off the West coast of Norway since 2009 were used as the main input to the simulations. Electricity price data from the same region and time periods were also used as input to further increase the realism of the results.

The main novelty of this study is the combination of using a detailed mathematical water electrolyzer simulation model together with operational data (from five different 31-day periods) from an actual FOWT installation, and the use of actual electricity price data for the same time periods. Hence, the simulation results of hydrogen production and calculations of hydrogen production costs are highly realistic and relevant for industry stakeholders that are considering similar concepts today (2023). This "real-world" approach makes this study different from other published studies (ref. literature survey in Literature review), which mainly focus on estimating hydrogen production capacity and costs for future scenarios (e.g., in 2030 and 2050) using assumed cost reductions and efficiency improvements, or studies that use modelled or estimated values for wind power and/or electricity price instead of real-world data.

This paper is structured in the following way: Literature review contains a review of relevant literature, System design and model-based approach describes the system design and the simulation model, Description of the simulation cases describes the simulation cases, Results and discussion presents the results and discussion, while Conclusions and future work goes through conclusions and suggestions for future work.

Literature review

Several previous academic studies have investigated hydrogen production from offshore wind. In 2014, Meier [5] performed a techno-economic assessment of hydrogen production from offshore wind. A wind profile based on the operation of a wind farm was extrapolated to estimate yearly energy and hydrogen production. The author concluded here that it is technically possible to build large-scale hydrogen production platforms connected to offshore wind turbines, but that it is not economically viable [5]. In 2015, Loisel et al. [6] simulated hydrogen production from offshore wind power based on data from a weather station. Various hydrogen use cases were evaluated and the results show negative profit in all scenarios [6]. In 2020, Schnuelle et al. [7] modelled dynamic hydrogen production from both photovoltaic (PV) power and wind power. A techno-economic assessment was performed and the results show that the onshore wind cases achieved a higher efficiency and lower production cost than the offshore wind cases, while the PV cases were found to be quite competitive with the onshore wind cases [7]. McDonagh et al. [8] simulated hydrogen production from a 504 MW offshore wind farm. The results show that it is more profitable to sell electricity directly to the grid instead of producing hydrogen. However, if hydrogen is produced it is most profitable to use a hybrid system that produces hydrogen from wind energy that would otherwise be curtailed [8].

In 2021, several more studies on wind/hydrogen systems were performed. Nguyen Dinh et al. [9] developed a model to assess the viability of hydrogen production from dedicated offshore wind farms. The case study was a hypothetical 101.3 MW wind farm, and the results show that the wind-hydrogen farm would be profitable in 2030 with a hydrogen price of 5 €/kg H_2 and underground storage capacity between 2 and 45 days [9]. Calado and Castro [10] reviewed the current state-of-the-art and future perspectives of hydrogen production from offshore wind, and both offshore and onshore hydrogen production was evaluated. The results show that the offshore alternative may be advantageous due to lower capital cost and transmission loss with gas pipelines vs. power cables. The advantage with the onshore alternative was more economic flexibility since it could sell both hydrogen and electricity [10]. Song et al. [11] analyzed future hydrogen production from offshore wind in China and delivery to Japan. Offshore wind power production was modelled based on meteorological data and hydrogen production and cost were estimated. The results show that it will be possible for China to supply the necessary amount of hydrogen at a cost consistent with Japan's future cost targets [11]. Ibrahim et al. [12] assessed large-scale hydrogen production from offshore wind power and considered three typologies: (1) Centralized onshore electrolysis, (2) Centralized offshore electrolysis and (3) Decentralized offshore electrolysis. It was here concluded that the offshore alternatives with hydrogen transport through pipelines to shore would be economical for large and distant offshore wind farms, while the advantage with the onshore alternative mainly would be the reduced complexity of the system [12]. Settino et al. [13] performed simulations of a system where a hydro-pneumatic energy storage device was used as a buffer between an offshore wind turbine and a hydrogen electrolyzer. The results show that an energy buffer can potentially reduce the on/off cycles of the electrolyzer by up to 70% with no substantial effect on the hydrogen production [13]. Scolaro and Kittner [14] investigated whether an offshore wind/hydrogen system would be cost-competitive in an ancillary service market and determined the optimal size of the hydrogen electrolyzer relative to the offshore wind farm. The results show that a carbon abatement cost between 187 and 265 €/ton CO_2 was needed to achieve profitability. The lowest cost occurred when the electrolyzer capacity was 87% of the wind farm capacity [14]. Lucas et al. [15] performed a techno-economic analysis of onshore hydrogen production from offshore wind power by using the Portuguese *WindFloat* Atlantic offshore wind farm as a case study. Two different wind farm capacities (25.2 MW and 150 MW) and two different hydrogen production cycles (24-h production and production only at night) were analyzed. The results show that only the scenario with 150 MW wind power and 24-h hydrogen production is economically feasible. This resulted in a hydrogen production cost of 4.25 €/kg H_2, and the minimum cost was achieved when the electrolyzer capacity was 30% of the wind farm capacity [15]. Tebibel [16] proposed a multi-objective optimization approach for a system with decentralized hydrogen production from onshore wind power. Wind data were used as input to a simulation model of a decentralized system consisting of a 857.5 kW wind turbine, a 250 kW alkaline electrolyzer, a 719 kW h battery and a 2022 kg hydrogen tank. The results show that the system can produce 8760 kg hydrogen per year. The estimated levelized cost of hydrogen (LCOH) for this system was 33.70 $/kg H_2, while the CO_2 emissions avoided were 87.75 ton/year [16].

Several studies of systems combining offshore wind power and hydrogen production were also published in 2022. Jang et al. [17] analyzed different scenarios for hydrogen production from offshore wind power, including both offshore (centralized and distributed) and onshore hydrogen production. The simulated system included a PEM electrolyzer and a 160 MW wind farm, and a 50% electrolyzer capacity factor was assumed. The results show that distributed offshore hydrogen production achieved the lowest cost when the cost of the wind farm was included, with a cost of 13.81 $/kg H_2. When the wind farm cost was excluded, the lowest cost achieved was the onshore hydrogen production scenario with a cost of 4.16 $/kg H_2. The offshore systems can become profitable with a hydrogen selling price of 14 $/kg H_2, while the onshore system would need a price of 16 $/kg H_2 to become profitable [17]. Luo et al. [18] reviewed possibilities for hydrogen production from offshore wind power in South China with the same scenarios used in Ref. [17]. It is concluded that distributed offshore hydrogen production using PEM electrolyzers is the most promising scenario. The total cost of a 400 MW wind farm with hydrogen production located 60 km offshore was estimated to be CNY2.7 billion, and a comparison analysis shows that it will be more advantageous to sell hydrogen and oxygen from a system of this type than to sell the electricity directly without subsidies [18]. Baldi et al. [19] analyzed hydrogen and ammonia-based pathways for storage, transportation and final use of excess electricity from an offshore wind farm. Wind speed data were used to estimate wind power production and real-world electricity price data

were used to estimate electricity price. It was concluded that it is currently more convenient to sell the electricity from offshore wind farms directly to the grid. The results show that hydrogen can be a viable option with a hydrogen price of 0.08 £/kWh and a renewable energy grid penetration of 60%. With a hydrogen price of 0.10 £/kWh or higher it will be favorable to produce hydrogen with an installed wind power grid penetration above 40% [19]. Benalcazar and Komorowska [20] analyzed the prospects for green hydrogen production from PV power and onshore wind in 2022, 2030, and 2050. The results from their techno-economic analysis show that the LCOH in Poland would be in the range 6.37–13.47 €/kg H_2 in 2022, 2.33–4.30 €/kg H_2 in 2030, and 1.23–2.03 €/kg H_2 in 2050 [20]. Lamagna et al. [21] modelled the hydrogen production from a reversible solid oxide fuel cell (SOFC) coupled to an offshore wind farm. Wind speed data and the average electricity price in Sweden in 2021 were used as input to a model that included a reversible SOFC, a sea water desalination plant and an energy management system. It was estimated that the hydrogen system can be placed inside a wind turbine using less than 2% of the turbine tower volume. For a large-scale wind farm, it was estimated that this solution would use 9.82% of the produced wind energy to produce hydrogen at a LCOH of 1.95 $/kg H_2 and a levelized cost of storage (LCOS) of 401 $/MWh [21]. Nasser et al. [22] performed a techno-economic assessment of hydrogen production from PV and wind power at different locations. Climatic data for wind speed, temperature, and solar radiation for each location were used as input to a model of an alkaline electrolyzer that simulated hydrogen production. The system efficiency (including PV and wind turbine efficiencies) was calculated to be in the range 7.69–9.37%, and the LCOH was calculated to be in the range 4.54–7.48 $/kg H_2 for the different locations [22]. Corengia and Torres [23] presented an optimization framework to design hydrogen production processes using grid electricity with or without the addition of wind and/or solar power. Electricity price data and public power data were used as input to a hydrogen production system model where both commercially available and possible future electrolyzer technologies were included. When only commercially available technologies can be used it was concluded that alkaline electrolyzers are a better choice than PEM electrolyzers, since the flexibility of the latter does not fully compensate for the added cost. If any electrolyzer technology can be used (including those not yet commercially available), the optimal solution would be to use a solid oxide electrolyzer (SOEL), either alone or in combination with alkaline electrolyzers and/or batteries, due to the high efficiency of SOELs and their expected relatively low future costs [23]. Groenemans et al. [24] performed a techno-economic analysis of hydrogen production from offshore wind power using PEM electrolysis. Wind data and the power curve of a 14 MW wind turbine were used to estimate wind power production and two hydrogen production scenarios were analyzed: (1) Hydrogen is produced offshore and transported to shore through a gas pipeline and (2) Electricity from an offshore wind farm is transported to shore through a power cable and hydrogen is produced onshore. The results show that the LCOH will be lower with offshore hydrogen production and can be as low as 2.09 $/kg H_2, while the estimated LCOH for the onshore scenario is 3.86 $/kg H_2 [24].

The interest in the combination of offshore wind and hydrogen systems is increasing rapidly and several new studies have already been published in the first quarter of 2023. Dinh et al. [25] developed a geospatial method to estimate the LCOH for a system that produces hydrogen through offshore electrolysis with electricity from offshore wind farms. Distance to port, water depth, distance to hydrogen pipeline injection point and wind characteristics of different locations were used as model inputs. The results show that the LCOH in 2030 varied by more than 50% between the locations; hence, the choice of location for these systems will be crucial for the viability of the concept. A 510 MW system in the best location in 2030 could produce up to 50 000 tons of hydrogen per year with a LCOH below 4 €/kg H_2 [25]. Komorowska et al. [26] analyzed future offshore wind-to-hydrogen production for several locations using a Monte Carlo-based framework. The results show that LCOH values can be in the range 3.60–3.71 €/kg H_2 in 2030 and 2.05–2.15 €/kg H_2 in 2050, with electricity prices and electrolyzer utilization rates having the greatest impact on the LCOH. An analysis of onshore wind-to-hydrogen systems was also performed and the results show that these systems can achieve a lower LCOH in the range 2.72–3.59 €/kg H_2 in 2030 and 1.17–1.36 €/kg H_2 in 2050 [26]. Kim et al. [27] analyzed the feasibility of offshore wind turbines linked with hydrogen production via electrolysis for different combinations of location, offshore distance, hydrogen/electricity transport method, electrolyzer location and electrolyzer type. The results show that offshore hydrogen production and transportation through gas pipelines is generally the most economical option when the distance to shore exceeds 100–200 km, while electricity transport through cables and onshore electrolysis is more economical when the distance to shore is shorter than 15 km. For the distances in between, the choice will depend on the other variables, e.g., windspeed and electrolyzer type. The unit cost ranges were estimated to be 1.64–3.13 $/kg H_2 for alkaline electrolyzers, 2.27–4.17 $/kg H_2 for PEM electrolyzers, and 3.43–4.46 $/kg H_2 for SOELs [27]. Gea-Bermúdez et al. [28] performed optimization modeling of the Northern-central European energy system and the North Sea offshore grid towards 2050 to evaluate whether it will be most beneficial to produce hydrogen (via water electrolysis) onshore or offshore. The main conclusion was that offshore wind power has a higher socio-economic value when it is transported to shore through power cables than when it is used to produce hydrogen offshore. Here it was shown that hydrogen can play a significant role in the future energy system in Europe, and that it should in most cases be produced onshore so that the flexibility of hydrogen as an energy carrier/energy storage can be fully utilized. If hydrogen production is forced offshore it can lead to an increase in total energy system cost of 9–28 billion $€_{2016}$/year by 2045 and an increase in emissions of 77–255 million tons of CO_2 in the period from 2020 to 2050 [28]. Durakovic et al. [29] used the open-source model EMPIRE [30] to model the European power grid towards 2060, and specifically how investments in green hydrogen production in and around the North Sea will impact European grid infrastructure and electricity prices. The results indicate that North Sea hydrogen production hubs can reduce the curtailment of offshore wind power in the region from 24.9% to 9.6%. In this study it was found that the impact on electricity prices by large-scale hydrogen production can be very different from country to

country. For example, the yearly average electricity price in Norway is estimated to increase significantly with hydrogen production, while the yearly average price in France and Germany is not expected to increase at all [29]. Kumar et al. [31] reviewed future opportunities related to synergies between large-scale hydrogen systems and various offshore industries. The study shows that small-scale offshore hydrogen production from excess renewable energy is economically unfeasible, while large-scale systems could be economically competitive if the conditions are favorable, i.e., low renewable electricity cost, high utilization factor for the electrolyzer and secure long-term hydrogen demand [31]. Li et al. [32] performed a techno-economic analysis of a simulated hybrid energy system that produces both electricity and hydrogen by using 120 MW of wind turbines, 80 MW of PV cells, 20 MW of batteries and 60 MW electrolyzer capacity. The results show that the renewable electricity production was 584.62 GW h per year, while the hydrogen production was 7432.71 ton/year with an electrolysis ratio of 22.31% and a LCOH of 13.1665 CNY/kg H_2 [32]. Giampieri et al. [33] performed a techno-economic analysis of hydrogen production from offshore wind power. Wind data and the power curve of a wind turbine were used as inputs to a model that calculated future hydrogen production capacity and cost for different scenarios. The results show that the most cost-effective scenario for 2025 would be offshore hydrogen production with pipeline transport, which could achieve a LCOH of 4.53 £/kg H_2 if the distance to shore is not more than 1000 km [33]. Nasser and Hassan [34] analyzed technical, economic, and environmental aspects of hydrogen production via electrolysis powered by PV cells, wind turbines, and waste heat. Weather data were combined with mathematical models to estimate electricity and hydrogen production. The results show large variations in LCOH between 1.19 and 12.16 $/kg H_2. The lowest cost was achieved when hydrogen was produced from waste heat, followed by grid power, PV cells and wind turbines [34]. Cheng and Hughes [35] analyzed the potential role for offshore wind power in renewable hydrogen production in Australia in 2030. Wind data, solar irradiation data and the power curve of a wind turbine were used as input to a model that simulated hydrogen production via PEM electrolysis, which resulted in an estimated LCOH range of 4.4–5.5 AUD/kg H_2 in 2030. The Australian target of 2 AUD/kg H_2 target could be reached if electrolyzer costs are reduced by 80% and the renewable electricity cost is around 20 AUD/MWh [35].

System design and model-based approach

The system simulation model used in this paper was developed and implemented in MATLAB/Simulink [36]. An overview showing the main components of the hydrogen system modelled in this paper is shown in Fig. 1, while a schematic of the Simulink model is shown in Fig. 2.

The Simulink model was built to simulate an energy system where the electricity from an offshore wind turbine is used to produce hydrogen via water electrolysis. The wind power and wind speed data used as input to the Simulink model are from a 2.3 MW floating offshore wind turbine (FOWT) called *Zefyros* and owned by the Norwegian company UNITECH Offshore AS [37], while the electricity price data were downloaded from Nord Pool [38]. Further details regarding the data sets are provided in Input data. A detailed mathematical model of a proton exchange membrane (PEM) electrolyzer was developed as part of a master's thesis at the University of Oslo [39], in close collaboration with researchers at the Institute for Energy Technology (IFE) that have modeling and experimental experience with PEM water electrolyzer systems [40,41]. This model was then slightly modified for use in this study. In addition to the PEM electrolyzer model, the Simulink model in this study includes a simple control system that regulates the energy flows, a lithium-ion battery system (standard Simulink component), as well as calculations of efficiency, energy use and cost of the various system components. These calculations are based on the values listed in Table 1. More detailed descriptions of the different sections of the model are given in the subsequent sections and in the Supplementary Information.

Assumptions and boundaries for the model

The Simulink model used in this study includes a detailed mathematical model of a PEM electrolyzer, described in PEM electrolyzer. The rest of the model components (balance of plant and economics) are kept very simple to minimize the complexity and computational load of the model. Balance of plant (BoP) includes the lithium-ion battery (standard Simulink component), as well as simple estimations of energy usage and cost for compression and storage of hydrogen and desalination of sea water. However, other BoP components (e.g., power electronics) are not included in the model. The exception is the cost estimate for the PEM electrolyzer which does include BoP (see Table 1). This means that the hydrogen production would most likely be lower in a real-world system since there is energy loss associated with power electronics. This would also increase the hydrogen production cost and decrease the overall efficiency. Furthermore, ramp-up time and cold start-up time for the PEM electrolyzer are not included in the model. However, according to Ref. [43], warm start-up (ramp-up) time for state-of-the-art PEM electrolyzers is less than 10 s, so the exclusion of this feature in the model should not have a great effect on the results. However, the cold start-up time is 5–10 min [43], which could influence the total hydrogen production. This effect would probably be most noticeable for high-capacity electrolyzers since the switch-off limit for the electrolyzers increases with increasing electrolyzer capacity. This effect would also be more noticeable in periods with low and variable wind power input since this increases the number of times the electrolyzer is switched off. A possible remedy to this challenge would be to use power from the onshore grid to keep the electrolyzer in standby mode and thereby avoid any cold start-ups, but this is not considered in this study. Any energy usage to keep the electrolyzer in standby mode is not included in the model. PEM electrolyzer–Control system and the Supplementary Information gives more detailed descriptions of the components included in the model.

The values for energy usage, water usage, costs, efficiency, and lifetime used in the model are listed in Table 1. The electrolyzer CAPEX includes power electronics and balance of plant (BoP).

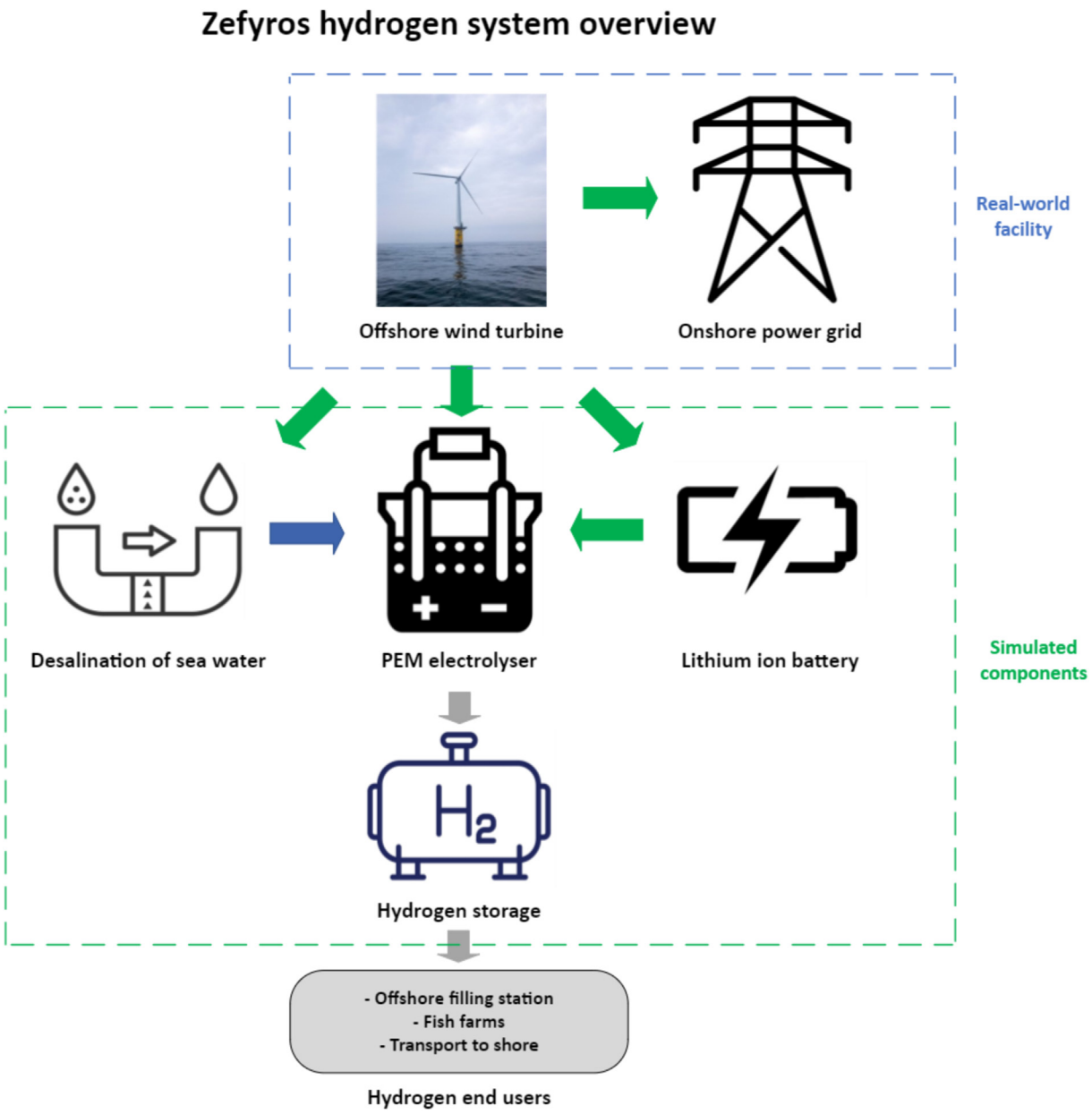

Fig. 1 – Overview of the Zefyros wind/hydrogen system. The real-world facility consists of the components inside the blue dashed box, while the components inside the green dashed box are simulated in MATLAB/Simulink. The green arrows indicate electricity flows, the blue arrow indicates water flow and the grey arrows indicate hydrogen flows. The hydrogen end users are suggestions and are outside the scope of this paper. The picture of the Zefyros wind turbine is courtesy of UNITECH Offshore AS [37] and all other icons are from Shutterstock [42]. (For interpretation of the references to colour in this figure legend, the reader is referred to the Web version of this article.)

PEM electrolyzer

A simplified structure of the proposed PEM electrolyzer model is shown in Fig. 3.

The PEM water electrolyzer model is divided into multiple modules, varying in complexity, where the top layer represents the initial conditions for the electrolyzer and the subsequent layers respond to the information generated by the previous modules. The thermal model, which influences all subsequent operating conditions, has a feedback loop. This is due to the stack temperature varying over time and its dependence on the previous and present model inputs. In the proposed model, the electrical response is assumed to be instantaneous, which will lead to behavior deviations from an actual PEM electrolyzer, especially during rapid changes in model inputs. The thermal model is described in more detail in the Supplementary Information available in the online version of this paper.

Product pressure

The pressure on the cathode and anode side of the membrane will be higher than the actual pressure measured in the

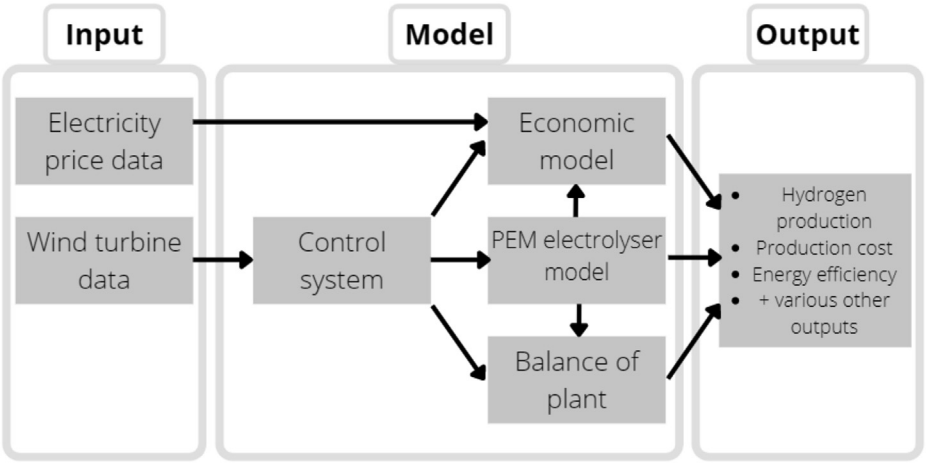

Fig. 2 – Schematic of the Simulink model used in all simulations.

Table 1 – Values used in modeling cases.

Parameter	Value
Desalination of sea water energy usage	4 kW h/m^3 [44]
Desalination of sea water cost	1.26 $/m^3 [44]
Desalination water amount	283.2 L/h per MW of electrolyzer power [45]
Lithium-ion battery round-trip efficiency	95% [46]
Lithium-ion battery CAPEX	469 $/kWh [47]
Lithium-ion battery OPEX	10 $/kW per year [47]
Lifetime of lithium-ion battery	10 years [47]
Hydrogen compression and storage cost	1.73 $/kg H_2 [48]
Hydrogen compression and storage energy usage	4 kW h/kg H_2 [48]
PEM electrolyzer (incl. BoP) CAPEX	1800 $/kW [49]
PEM electrolyzer (incl. BoP) OPEX	5% of CAPEX per year [43]
Lifetime of PEM electrolyzer	100 000 h [43]
Cost of platform for electrolysis, desalination and compression	3 000 000 $/MW of PEM electrolyzer power [44]
Lifetime of platform for electrolysis, desalination, and compression	40 years [44]

product flow channels due to supersaturation in the different layers. The pressures of the products (O_2 and H_2) are also proportional to the current density since it dictates the production rate. The oxygen pressure at the anode side is calculated as the sum of the anode pressure, which is set to 1 bar, and a partial pressure increase factor, minus the vapor pressure of water. This is described in equation (1) [50]:

$$P_{O_2} = P_{an} + \gamma_{O_2} \cdot i - P^{vp}_{H_2O} \quad [bar] \tag{1}$$

Where i is the current density, $P^{vp}_{H_2O}$ is the vapor pressure of water, and the empirical parameter γ_{O_2} is the partial pressure increase factor for an IrO_2 catalyst layer [50].

The hydrogen pressure at the cathode side is calculated as the sum of the cathode pressure, which is set to 30 bar, and the partial pressure increase factor for hydrogen, minus the vapor pressure of water [50]:

$$P_{H_2} = P_{cat} + \gamma_{H_2} \cdot i - P^{vp}_{H_2O} \quad [bar] \tag{2}$$

Cell voltage

The operating potential of the cell during different conditions must be known to calculate the efficiency of the electrolyzer. The cell voltage can be described as the sum of the open-circuit voltage U_{OCV} and three voltage overpotentials: $U_{activation}$, U_{ohmic} and $U_{concentration}$, as seen in equation (3) [51]:

$$U_{cell} = U_{OCV} + U_{act} + U_{ohm} + U_{con} \quad [V] \tag{3}$$

Open-circuit voltage. The Open-Circuit Voltage (OCV) is a measurement of the potential between the two electrodes in the cell. This is often expressed as the sum of the reversible cell voltage and an expression that relates the activity of the products to the reactants involved in the process. The activity of products and reactants is closely related to the concentration of the species and can be expressed through the species' relative pressure difference. The OCV for constant pressure conditions can be described through a modified Nernst equation [51]:

$$U_{OCV} = U_{rev} + \frac{R \cdot T}{2 \cdot F} \ln\left(\frac{P_{H_2}}{P_{cat}} \sqrt{\frac{P_{O_2}}{P_{an}}}\right) \quad [V] \tag{4}$$

Where U_{rev} is the reversible voltage [52,53], R is the ideal gas constant, T is the cell temperature in Kelvin, and F is the Faraday constant.

Activation overpotential. The activation overpotential represents the energetic barrier that needs to be surpassed in order to begin the electrochemical reaction. The total activation overpotential can be expressed as the sum of the anode and cathode activation overpotential, shown in equation (5) [52,54]:

$$U_{act} = U^{an}_{act} + U^{cat}_{act} \quad [V] \tag{5}$$

A catalyst reduces the activation barrier, and thereby decreases the potential that needs to be applied. The anode and cathode activation overpotential can be further described

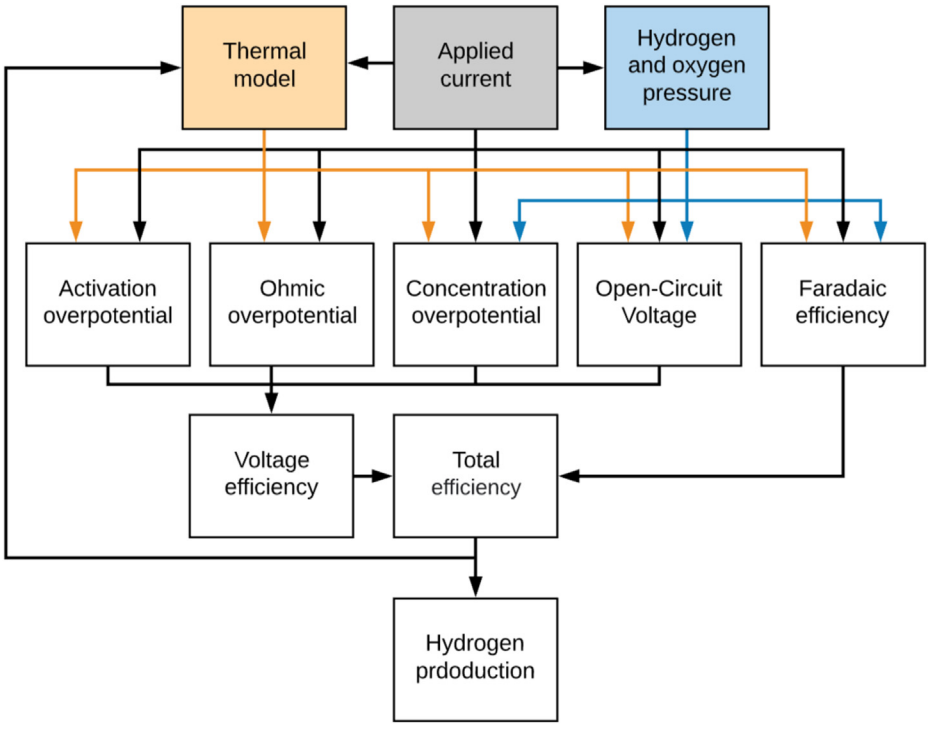

Fig. 3 – Schematics of the proposed PEM electrolyzer model [39].

using the Butler-Volmer equation, shown in equations (6) and (7) for the anode and cathode [51,52,54–56]:

$$U_{act}^{an} = \frac{R \cdot T}{\alpha_{an} \cdot F} \operatorname{arcsinh}\left(\frac{i}{2 \cdot i_{0,an}}\right) \quad [V] \tag{6}$$

$$U_{act}^{cat} = \frac{R \cdot T}{\alpha_{cat} \cdot F} \operatorname{arcsinh}\left(\frac{i}{2 \cdot i_{0,cat}}\right) \quad [V] \tag{7}$$

Where i is the current density, i_0 is the exchange current density and α is a dimensionless charge transfer coefficient. It is common to assume symmetrical behavior between the anode and cathode side, resulting in $\alpha_{an} = \alpha_{cat} = 0.5$ [52,54,55,57], and this assumption is used in this study. The exchange current density is calculated using an expression based on the Arrhenius equation [52,55–58].

Ohmic overpotential. The ohmic overpotential is simplified in the proposed model and contributes only to the ionic loss in the membrane, since the membrane is the dominant source of resistance in the cell. The ohmic overpotential caused by the membrane can be expressed through equation (8) [51,52]:

$$U_{ohm} = \frac{\delta_{mem}}{\sigma_{mem}} i \quad [V] \tag{8}$$

here δ_{mem} is the membrane thickness, i is the current density and σ_{mem} is the membrane conductivity, which can be calculated using an empirical expression for Nafion™ membranes [52].

Concentration overpotential. The concentration or diffusion overpotential arises due to variations in reactant concentration at the electrode surface, both at the anode and cathode side. This occurs when the current density is high enough to impede the surface reaction by overpopulating the membrane with gas bubbles and thereby slowing down the reaction rate. The concentration overpotential is the sum of the contribution at both the anode and the cathode side [52]:

$$U_{con} = U_{con}^{an} + U_{con}^{cat} \quad [V] \tag{9}$$

In order to express the voltage loss due to a surplus of reaction products, the Nernst equation can be combined with Fick's law, which gives an equation valid for static cell pressure. This expression is given in equations (10) and (11) for the anode and cathode side respectively [50,52]:

$$U_{con}^{an} = \frac{R \cdot T}{4 \cdot F} \ln\left(\frac{P_{O_2}}{P_{an} - P_{H_2O}^{vp}}\right) \quad [V] \tag{10}$$

$$U_{con}^{cat} = \frac{R \cdot T}{2 \cdot F} \ln\left(\frac{P_{H_2}}{P_{cat} - P_{H_2O}^{vp}}\right) \quad [V] \tag{11}$$

Efficiency

The electrical efficiency of the electrolyzer can be expressed by multiplying the Faradaic efficiency and voltage efficiency, as shown in equation (12) [59]:

$$\eta_{tot} = \eta_F \cdot \eta_V \quad [\%] \tag{12}$$

The voltage efficiency η_V is defined by equation (13) [59]:

$$\eta_V = \frac{Thermal\ neutral\ voltage}{Operating\ cell\ voltage} = \frac{U_{th}}{U_{cell}} = \frac{1.481}{U_{cell}} \quad [\%] \tag{13}$$

The Faradaic efficiency, also referred to as the Coulomb efficiency or current efficiency, defines the efficiency of charge transfer in an electrolyzer. For a PEM electrolyzer this is effectively the efficiency of oxygen production at the anode

side and the hydrogen formation at the cathode side. This can be expressed in terms of current density [60]:

$$\eta_F = 1 - \frac{i_x}{i} \quad [\%] \tag{14}$$

Where i_x is the total gas crossover current density [60], which is a sum of the hydrogen and oxygen crossover current densities.

Hydrogen production

The power consumed by the electrolyzer stack can be expressed through Ohm's law, shown in equation (15):

$$P_{in} = U_{cell} \cdot I \cdot N_{cell} \quad [W] \tag{15}$$

Where U_{cell} is the cell voltage, I is the current applied to the cell and N_{cell} is the number of cells in the electrolyzer stack. By knowing the power consumption and the electrolyzer efficiency it is possible to calculate the hydrogen production rate, shown in equation (16) [59,61]:

$$\dot{m}_{H_2} = \frac{P_{in} \cdot \eta_{tot}}{HHV_{H_2}} \quad \left[\frac{kg}{s}\right] \tag{16}$$

Where $\dot{m}_{H_2}$ is the hydrogen production rate and HHV_{H_2} is the higher heating value of hydrogen in J/kg.

Balance of plant

Lithium-ion battery

The lithium-ion battery used in some of the simulation cases is the standard version available in the MATLAB/Simulink software package [36]. Adjustments of the energy and power capacities were made between the different cases. The energy storage capacity for the batteries was set to five times the charging/discharging power (e.g., a charging/discharging power rating of 200 kW gives an energy storage capacity of 1000 kW h). The charging/discharging power and energy storage capacities for the different system designs are shown in Table 3. With the state of charge (SOC) range set to 20–80% the battery can supply energy to the electrolyzer for approximately 3 h at a constant discharge power from 80 to 20% SOC. This means that the battery can only cover power demands over relatively short periods when the wind turbine is not producing enough power for the electrolyzer. Longer periods of low wind power production will require the electrolyzer to shut down. An alternative strategy could be to use power from the onshore grid to keep the electrolyzer running at minimum power (10%), but this has not been considered in this study. The charging/discharging and SOC conditions for the battery are described in Control system.

Hydrogen compression and storage

The hydrogen compression and storage section of the model calculates the energy usage and cost of this part of the system, based on the values listed in Table 1.

Desalination of sea water

The desalination section of the model calculates the energy usage, required water amount and cost of this part of the system, based on the values listed in Table 1.

Cost estimations

The economic section of this model uses the various cost values listed in Table 1 to estimate the production cost of hydrogen for each case. Investment and operating costs (CAPEX and OPEX) are calculated for the key system components, including a PEM electrolyzer, a lithium-ion battery, electricity from the grid, sea water desalination plant, hydrogen compressor, hydrogen storage, and an offshore platform for the electrolyzer and the BoP components. The total CAPEX for a system component is adjusted according to its expected lifetime by using the following method: Total CAPEX is divided by the expected lifetime and multiplied by the length of the simulation period (*Example*: The PEM electrolyzer has an expected lifetime of 100 000 h, so the total CAPEX is divided by 100 000 and multiplied by 744, which is the number of hours in the 31-day simulation period). The cost

Table 2 – The five different time periods used in the simulations. The electricity price is converted from NOK to US $ using 8.74 NOK/$, which was the conversion factor at the time the simulations were performed (February 2022).

Time period	Tag	Wind turbine capacity factor [%]	Average electricity price [$/kWh]
07.03–06.04.2020	A	63.6	0.0091
20.12.2020–19.01.2021	B	21.3	0.0440
01.01–31.01.2022	C	55.1	0.1609
01.06–01.07.2020	D	30.9	0.0018
01.12–31.12.2020	E	41.7	0.0245

Table 3 – Overview of the different system designs used in the simulations.

System design	Electrolyzer power [kW]	Combined electrolyzer and compressor power [kW]	Li-ion battery energy/power [kWh/kW]	Grid-connected
High capacity with battery (HC + B)	1852	2000	1000/200	Yes
Medium capacity with battery (MC + B)	926	1000	500/100	Yes
Low capacity with battery (LC + B)	463	500	250/50	Yes
High capacity without battery (HC)	1852	2000	No battery	Yes
Medium capacity without battery (MC)	926	1000	No battery	Yes
Low capacity without battery (LC)	463	500	No battery	Yes

estimations used in the model do not include discount rate. This will be a subject of future work.

Input data

Measured data for wind power production and wind speed from a 2.3 MW FOWT are used in all models. Five different time periods are used, each lasting 31 days. The time periods are listed in Table 2 together with the simulation cases. All data sets have data points with 10-min intervals, except the data set from 2022 which uses 60-min intervals. The data points give the average value for the given time periods. The data sets from the FOWT are the property of the Norwegian company UNITECH Offshore AS [37] and are not publicly available currently.

Electricity price data from Nord Pool [38] for the five simulation periods are also used as input to the models. These data sets are used to calculate the electricity cost, which is part of the production cost of hydrogen for the system. Nord Pool uses data points with 60-min intervals, and this is used as the average electricity price for each hour in the models. The Nord Pool data is publicly available for download on their website [38].

Control system

Main principle

The control system is based on simple logical switches and relational operators that decide when the various components should receive energy from the wind turbine. These decisions are made based on the magnitude of the incoming wind power and the preset capacities of the various components. The electrolyzer operates when the wind power is $\geq$ 10% of the combined rated power of the electrolyzer and hydrogen compressor. If the wind power is < 10% then either a battery is used or the electrolyzer is switched off. This is to avoid excessive on/off-switching of the electrolyzer when the wind turbine fluctuates in the low power range around its cut-in wind speed. The hydrogen production in this lower power range would in any case be very small, and this power should therefore instead be exported to the electricity grid. Illustrations of the control systems for the simulation cases with and without battery is shown in Figs. 4 and 5, respectively.

Electrolyzer

The electrolyzer produces hydrogen if the power delivered from the wind turbine is more than or equal to 10% of the combined rated power of the electrolyzer and hydrogen compressor. *Example:* If the combined rated power of the electrolyzer and compressor is 2000 kW, the electrolyzer produces hydrogen if the power delivered from the wind turbine is 200 kW or higher.

If the power delivered from the wind turbine is less than 10% of the combined rated power of the electrolyzer and hydrogen compressor, there are several alternatives.

- If the system includes a battery and the battery state of charge (SOC) is higher than 20%, the battery delivers power to the electrolyzer and compressor equal to 10% of their rated power.
- If the system includes a battery and the battery state of charge (SOC) is *not* higher than 20%, the electrolyzer is switched off.
- If the system does *not* include a battery, the electrolyzer is switched off.

Battery

If the system includes a battery, the charging/discharging rules are as follows.

- The round-trip efficiency of the lithium-ion battery is assumed to be 95% [46] and this is applied to the charging of the battery with power from the wind turbine. The power to charge the battery is set to be constant and equal to 10% of the combined rated power of the electrolyzer and hydrogen compressor, divided by 0.95 to include the efficiency of the lithium-ion battery. *Example:* If the combined rated power of the electrolyzer and hydrogen compressor is 2000 kW, the battery will be charged with a power equal to 200/0.95 kW = 210.53 kW
- The SOC range of the lithium-ion battery is set to be 20–80%, i.e., charging is switched off when the SOC reaches 80% and discharging is switched off when the SOC gets down to 20%.
- If the power from the wind turbine is lower than 10% of the combined rated power of the electrolyzer and hydrogen compressor, *and* the battery SOC is higher than 20%, the battery discharges (supplies power to the electrolyzer and compressor) with a power equal to 10% of the combined rated power of the electrolyzer and hydrogen compressor until the SOC is at 20%.*Example:* If the combined rated power of the electrolyzer and compressor is 2000 kW, then the battery delivers a total of 200 kW to the electrolyzer (185.2 kW) and compressor (14.8 kW) if the wind power is below 200 kW *and* the battery SOC is higher than 20%.
- If the power from the wind turbine is higher than the sum of the charging power of the battery and 10% of the combined rated power of the electrolyzer and hydrogen compressor, *and* the battery SOC is lower than 80%, the battery will be charged by wind power equal to the rated charging power of the battery. *Example:* If the combined maximum power of the electrolyzer and compressor is 2000 kW, then the battery will be charged with the charging power of 210.53 kW when the following conditions are met: The wind power is higher than 410.53 kW (200 kW to the electrolyzer and compressor and 210.53 kW to the battery) *and* the battery SOC is lower than 80%.

Desalination of sea water

If the power from the wind turbine is lower than 10% of the combined rated power of the electrolyzer and hydrogen compressor, then some of the wind power will be used to desalinate sea water for later use in the electrolyzer. The power requirement for desalination is very low so it is never an issue to have enough power for this purpose. In the case with the highest hydrogen production (case 4), 2.14 kW is the maximum power and 1.40 kW is the mean power used by the desalination system.

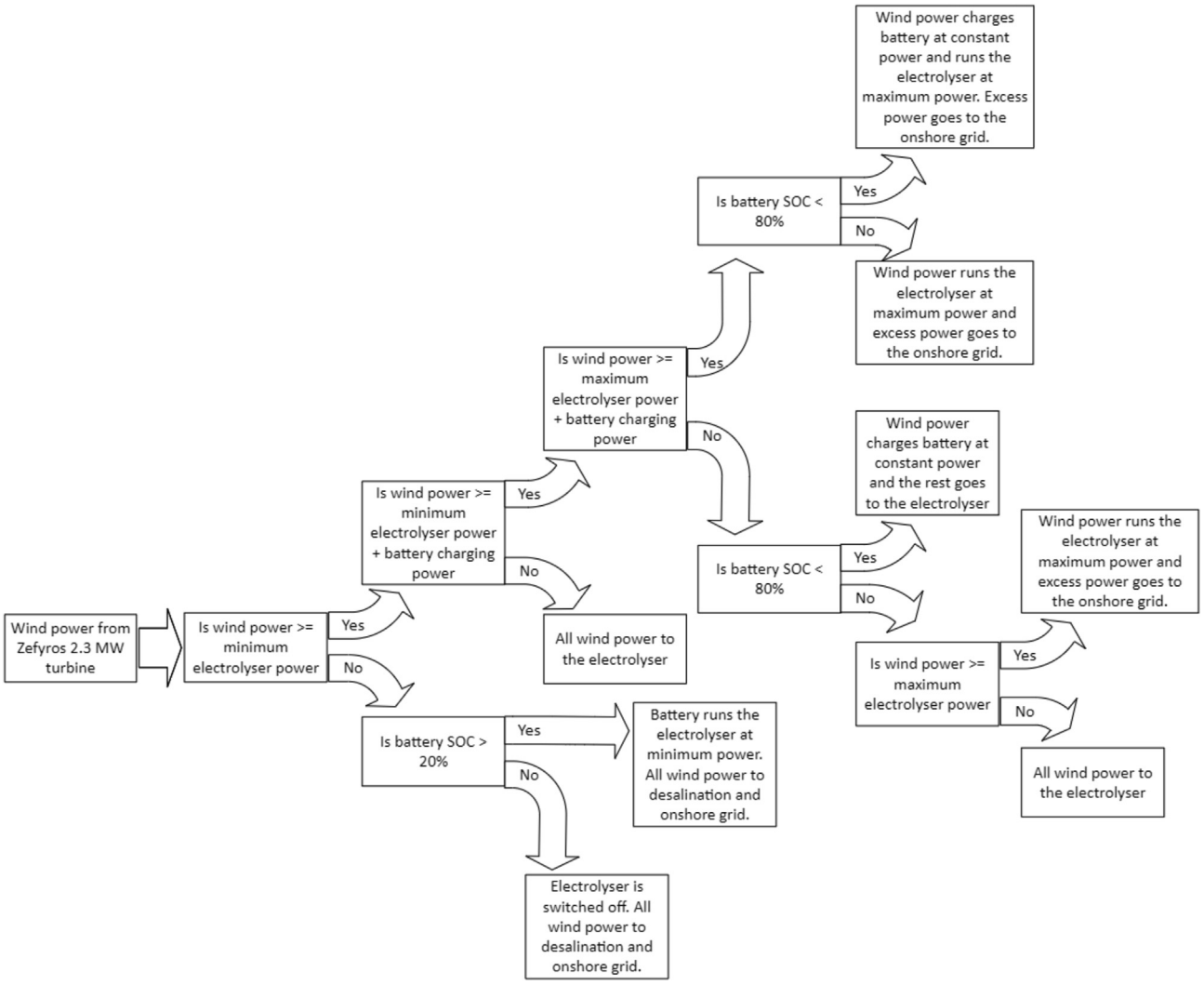

Fig. 4 – Overview of the control system for the simulation cases with a battery. The energy for compression and storage of hydrogen is deducted from the electrolyzer power when it is producing hydrogen, as explained in section *Control system*.

Compression and storage of hydrogen

The energy requirement of this part of the system is listed in Table 1, and the wind turbine delivers this power whenever the electrolyzer is producing hydrogen.

Onshore grid

There are two situations in which some of the wind power is delivered to the onshore grid.

- If the power from the wind turbine is higher than the combined rated power of the electrolyzer and hydrogen compressor, the excess wind power is delivered to the onshore grid, except in the cases that include a battery. In those cases, if the battery SOC is lower than 80%, the battery will be charged up to SOC 80% with some of the excess power. The rest is delivered to the onshore grid.
- If the power from the wind turbine is lower than 10% of the combined rated power of the electrolyzer and hydrogen compressor, the power from the wind turbine is delivered to the onshore grid after the power for the desalination of sea water has been subtracted.

Description of the simulation cases

In the case studies presented in this paper, real-world data from a 2.3 MW FOWT is used as input to a MATLAB/Simulink model to simulate hydrogen production from an offshore wind power system. The main outputs from the simulations are the hydrogen production capacity, production cost, and energy efficiency. The paper presents the results of 30 different simulations. These are divided into five different 31-day periods with six different system designs. The five time periods are listed in Table 2 and the system designs are listed in Table 3. Table 2 also gives the wind turbine capacity factor and the average electricity price for each period. The different time periods were chosen to compare time periods with different wind turbine capacity factors and electricity prices. These are by far the two most important factors for the

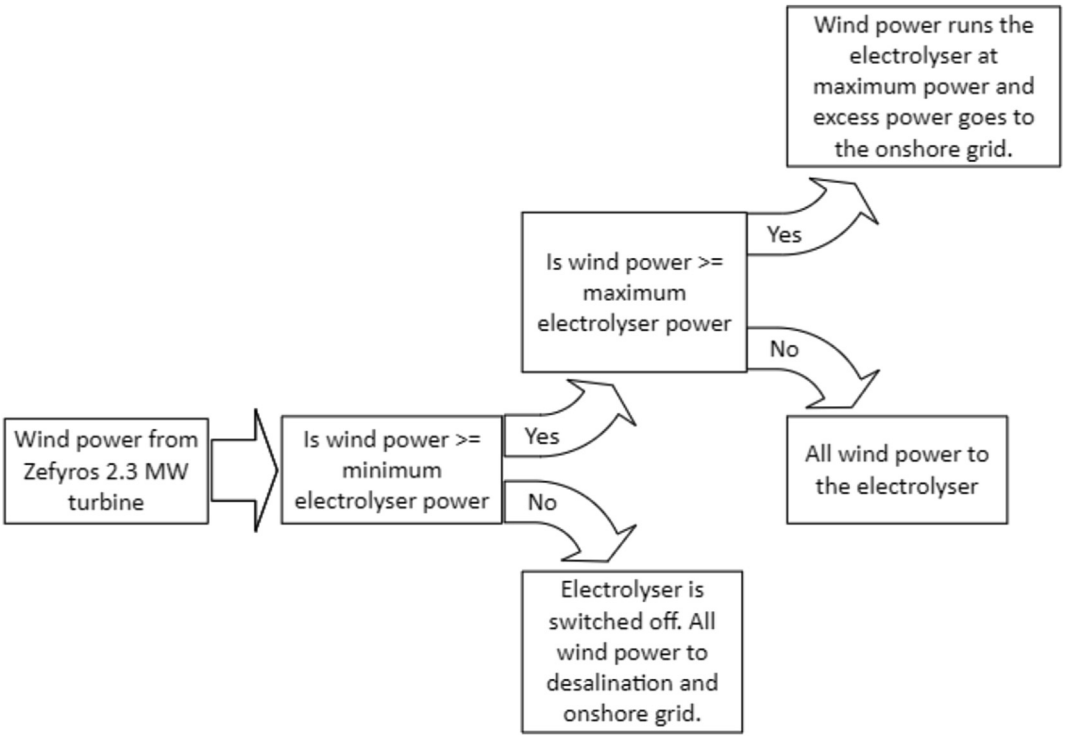

Fig. 5 – Overview of the control system for the simulation cases without a battery.

economic viability of a wind/hydrogen system, and the most favorable conditions are high wind turbine capacity factors and low electricity prices. A low electricity price is favorable because the opportunity cost of producing hydrogen versus selling the wind power as electricity increases with increasing electricity price (i.e., it is better to sell electricity than hydrogen when the electricity price is high).

From Table 2 it can be observed that time period A represents a nearly ideal period for hydrogen production since it has both a very high wind turbine capacity factor and a low electricity price. Period B represents a period with poor conditions for hydrogen production because of the very low wind turbine capacity factor. The electricity price in this period was relatively close to the long-term average price for the period 2016–2021, which was 0.0515 $/kWh (calculated using price data from Nord Pool [38]). Period C was chosen to include a period where both the wind turbine capacity factor and the electricity price is very high, while period D was chosen to include a period where both the capacity factor and electricity price were low. Period E was chosen to include a period where the wind turbine capacity factor was very close to the typical value for offshore wind turbines, and the electricity price was neither extremely high nor extremely low. Period E therefore represents the closest to what would be expected for an average month. However, it should be noted that the electricity price in Norway (where the turbine is located and connected to the grid) has fluctuated wildly in the past couple of years, from almost negative prices in the summer of 2020 to almost five times the long-term average price at the end of 2021 and beginning of 2022. Any electricity price predictions for the future are therefore exposed to extreme uncertainty.

Six different system designs were used in the simulations, and the specifications and abbreviations used are given in Table 3. The first three setups; high capacity with battery (HC + B), medium capacity with battery (MC + B), and low capacity with battery (LC + B) are cases where the electrolyzer and battery capacities are high, medium, and low compared to the maximum wind turbine capacity of 2.3 MW. The next three designs (HC, MC, and LC) are identical to the first three, except that they do not include a battery in the system.

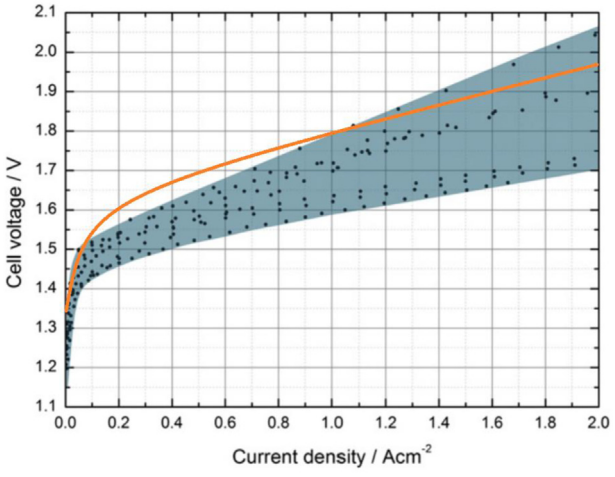

Fig. 6 – Single cell PEM electrolyzer voltage performance published in literature compared to the model in this study. The voltage performance of the model in this study (orange line) has been superimposed on the original figure from Carmo et al. [56]. (For interpretation of the references to colour in this figure legend, the reader is referred to the Web version of this article.)

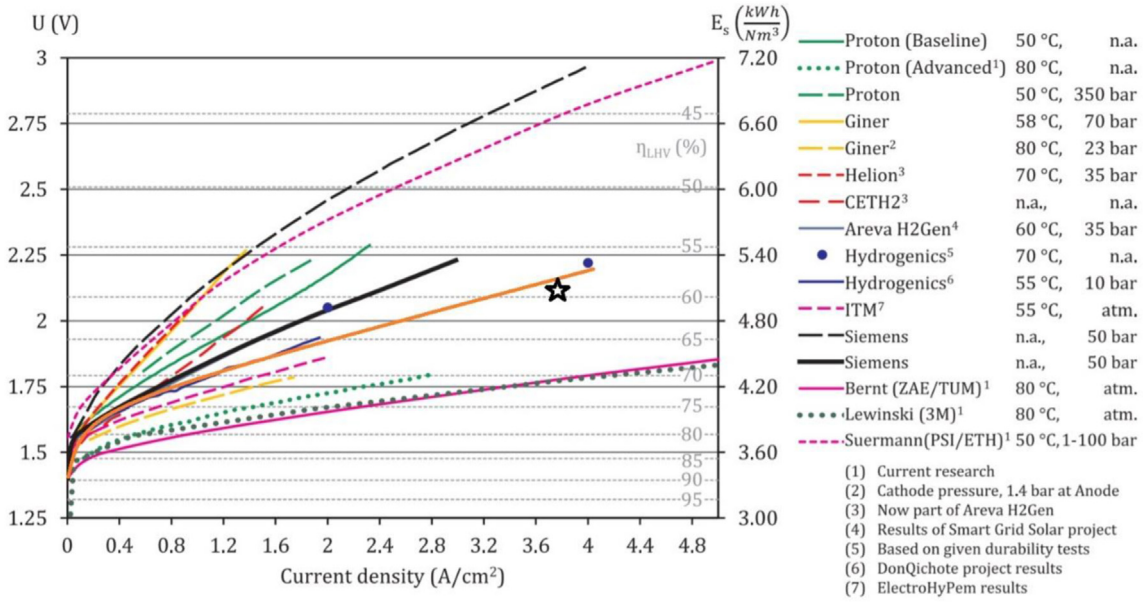

Fig. 7 – Reported commercial PEM electrolyzer voltage profiles compared to the voltage profile of the model in this study. The figure with previously published voltage profiles is taken from Ref. [43], and the voltage profile from this study is shown by the full orange line next to the black star. (For interpretation of the references to colour in this figure legend, the reader is referred to the Web version of this article.)

Results and discussion

Electrolyzer model validation

In order to validate the overpotential behavior of the model some comparison to published literature have been made. In Fig. 6 a range of published polarization curve results are given in the shaded area, and these are compared to the curve produced by the model in this study, which is shown by the orange curve.

The shaded area is a range of published polarization curves taken from Carmo et al. [56]. The results are gathered from published results between 2010 and 2012 for single PEM cells. The cells are reported to use an iridium-based catalyst for the anode and a platinum-based cathode catalyst. The cells utilize Nafion^{TM} membranes and are operating at 80 °C. The operating pressure is not disclosed. As seen from the figure, the modeling result in this study (illustrated by the orange line) are slightly higher than previously published results for current densities between 0.1 and 1 A/cm^2, and at the upper end of the range for current densities above 1 A/cm^2.

Fig. 7 shows a range of reported commercial PEM electrolyzer voltage performances compared to the profile from this study (the same profile used in Fig. 6).

As shown in Fig. 7, the voltage profile of the model in this study (full orange line next to the black star) is positioned near the middle of the range of the reported PEM electrolyzer voltage profiles from Ref. [43]. It can be noted here that most of the profiles that have a higher overpotential than the one for the model used in this study are operating at lower temperatures and higher pressures. Most of the voltage profiles that have a substantially lower overpotential are advanced electrolyzers operating at atmospheric cathode pressure.

Summary of simulation results

Table 4 lists all 30 simulation cases (scenarios) for the five time periods and six system designs, as well as the total hydrogen production, total production cost per kg of hydrogen, and overall system efficiency of each case.

Hydrogen production capacity

The total hydrogen production for all cases (Table 4 and Fig. 8) is, as expected, strongly affected by both the electrolyzer capacity (power) and the wind power production for the given time period. The inclusion of a battery has a negligible effect on the total hydrogen production. This can be seen by comparing the production in the cases with equal electrolyzer power in the same time period, where one case includes a battery and one does not (for example cases 1 and 4).

The total hydrogen production increases with increasing electrolyzer capacity, but the specific hydrogen production (kg/kW of rated electrolyzer power) is higher when the rated electrolyzer power is low. This can be seen in all time periods when comparing the hydrogen production for the different system designs in Table 4. For example, the hydrogen production per kW of electrolyzer power for cases 1, 2 and 3 are 9.3, 11.0 and 12.0 kg H_2/kW, and the same pattern can be seen for the other cases. This shows that the utilization of the electrolyzer capacity is higher in the systems with smaller electrolyzers. The reason for this is that the electrolyzers shut down when the wind power is lower than 10% of the combined rated power of the electrolyzer and hydrogen compressor, and this shut-down limit will be higher for the electrolyzers with higher rated power. Therefore, when comparing two electrolyzers with different power capacities during the same time period (with equal wind power

Table 4 – Overview of the main results from all wind/hydrogen system simulations. Case 4 is studied in more detail in section *In-depth study of case 4*.

Case	Time period	System design	Total H_2 production [kg]	H_2 production cost [$/kg H_2]	Efficiency of H_2 production (LHV) [%]
1	A	HC + B	17 218	5.46	56.6%
2	A	MC + B	10 158	4.98	56.7%
3	A	LC + B	5570	4.74	56.7%
4	A	HC	17 242	5.18	56.8%
5	A	MC	10 145	4.74	56.9%
6	A	LC	5561	4.53	56.9%
7	B	HC + B	5612	14.49	56.2%
8	B	MC + B	3841	11.75	56.4%
9	B	LC + B	2503	10.02	56.8%
10	B	HC	5649	13.57	56.7%
11	B	MC	3852	11.10	56.8%
12	B	LC	2497	9.55	56.8%
13	C	HC + B	15 016	13.91	56.6%
14	C	MC + B	9036	13.43	56.7%
15	C	LC + B	5020	13.23	56.8%
16	C	HC	15 041	13.61	56.8%
17	C	MC	9033	13.18	56.9%
18	C	LC	5009	13.00	56.9%
19	D	HC + B	8283	8.54	56.1%
20	D	MC + B	5963	6.50	56.5%
21	D	LC + B	3836	5.46	56.6%
22	D	HC	8353	7.91	56.7%
23	D	MC	5974	6.08	56.8%
24	D	LC	3833	5.15	56.8%
25	E	HC + B	11 298	8.09	56.7%
26	E	MC + B	6677	7.32	56.7%
27	E	LC + B	3676	6.93	56.8%
28	E	HC	11 296	7.66	56.8%
29	E	MC	6675	6.96	56.9%
30	E	LC	3671	6.61	56.9%

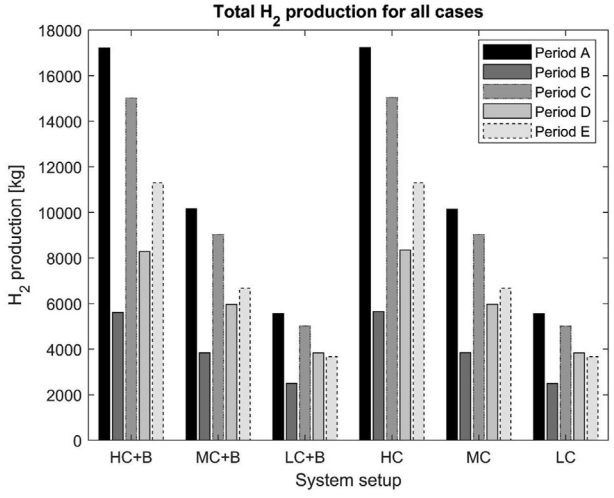

Fig. 8 – Overview of the total hydrogen production in all simulation cases. See Table 2 for information about the different time periods and Table 3 for explanation of the different system designs.

production), the electrolyzer with the highest rated power will have more downtime than the electrolyzer with the lowest rated power. Including a battery in the system has a negligible effect on this issue. However, if the objective is to maximize the total hydrogen production it is beneficial to have an electrolyzer with a rated power close to the rated power of the wind turbine. This is because the total hydrogen production will be much higher for the high capacity electrolyzers compared to the low or medium capacity electrolyzers, even though the high capacity electrolyzer has more downtime.

Hydrogen production cost

The production cost per kg of hydrogen for all cases is provided in Table 4 and illustrated in Fig. 9. It should be noted that the hydrogen production cost does not include the cost of the wind turbine, since the *Zefyros* wind turbine used in these simulation cases is a real turbine already in operation. The hydrogen production cost is therefore only the estimated cost of adding the hydrogen system to the existing turbine.

The hydrogen production cost is strongly affected by the wind turbine capacity factor and the price of electricity. The cases in the time period with the worst conditions (period B) yields hydrogen production costs 2–3 times as high as the period with the most favorable conditions (period A). As expected, this indicates that the profitability of this type of wind/hydrogen system would vary greatly from month to month. The use of a battery does not seem to reduce the production cost per kg hydrogen. In fact, the cases without batteries have consistently lower hydrogen production costs, i.e., adding batteries adds cost to the system without increasing the hydrogen production.

It should also be noted that a battery adds complexity to the system and should therefore not be included unless the

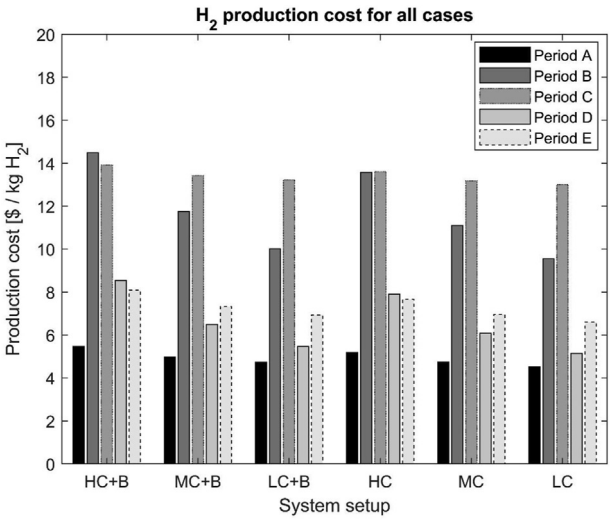

Fig. 9 – Overview of the hydrogen production cost in all simulation cases. See Table 2 for information about the different time periods and Table 3 for explanation of the different system setups.

results are significantly better with a battery than without. However, it should also be noted that the effect of including a battery might be different in a real-world system where the efficiency of the electrolyzer could be more affected by the fluctuating wind power than it is in this mathematical model. In the simulations in this study the efficiency of the PEM electrolyzer is never below approximately 70%, which might not be achievable in real-world systems with existing technology. Another possibility might be to use power from the onshore grid instead of a battery to smooth out the fluctuations in input power to the electrolyzer. These aspects are something that should be tested in future experimental work and are outside the scope of this study.

Other studies [62–65] summarized in Ref. [66] have estimated that the production cost of so-called "green hydrogen", i.e., hydrogen produced by electrolysis using electricity from renewable sources, with existing state-of-the-art technology is in the range 2.50–6.80 $/kg H_2 [66]. The cost when using wind power (only onshore) is in the range 4.22–5.76 $/kg H_2 [66]. When comparing the production cost of the simulation cases in this study with the sources above, all cases in period A fit very well within the estimated range for hydrogen production from wind power. The other periods suffer from a low wind turbine capacity factor and/or high electricity price and most of the cases are therefore well above the estimated upper value of 6.80 $/kg H_2 from Refs. [62,63]. All cases in period B (very low wind turbine capacity factor) and period C (very high electricity price) have production costs that are much higher than this upper value. Period D and E present more mixed results where some cases are within the estimated range and some cases are above.

Energy efficiency

The overall energy efficiency of the hydrogen production process is calculated by dividing the energy content of the produced hydrogen (using the lower heating value of hydrogen of 33.3139 kW h/kg H_2 [67]) by the wind energy input to the hydrogen system:

$$\eta = \frac{E_{H_2}}{E_{in}} \cdot 100\% = \frac{E_{H_2}}{E_{Zefyros} - E_{grid}} \cdot 100\% \quad (17)$$

The overall efficiency varies very little between the cases. The average efficiency is 56.6% and all cases have an efficiency that is in the range 56.1–56.9%, as shown in Table 4. Both the time period and the system design have very little effect on the overall efficiency. The reason for the small variation in efficiency is that the efficiency of all BoP components (battery, hydrogen compression and storage, desalination of sea water) is assumed to be constant (based on values listed in Table 1) and the dynamic efficiency of the PEM electrolyzer varies very little between the cases. The electrolyzer efficiency is described more closely in In-depth study of case 4. The overall efficiency is slightly reduced when a battery is included in the system. This is because the energy loss is assumed to be 5% [46] when the wind power goes through the battery before it is used to produce hydrogen, and since the total hydrogen production is almost unchanged this reduces the overall efficiency. The efficiency in a real-world system would fluctuate more and would most likely be lower than the estimates in this study due to the simplifications described above. The magnitude of the fluctuations and the difference in overall efficiency will be a subject of future work.

In-depth study of case 4

Simulation case 4 is a scenario where the wind turbine has a high capacity factor (63.6%) and the average electricity price is low (0.0091 $/kWh), and the wind/hydrogen-system is designed with the largest possible electrolyzer. The system does not include a battery. The results show that this was the case with the highest total hydrogen production (17 242 kg) and the hydrogen production cost of 5.18 $/kg H_2 is well within the estimated range of 2.50–6.80 $/kg H_2 [62–66] for green hydrogen. Hence, this is the most favorable case when assuming the main objective is to maximize hydrogen production at the lowest possible cost. As shown in Table 4 and Fig. 9, cases 5 and 6 have slightly lower production costs than case 4 due to less electrolyzer downtime (as explained in Summary of simulation results), so if the demand for hydrogen from the system is low it would be more economical to use a smaller hydrogen system.

The efficiency and input power of the electrolyzer during the first three days of operation in case 4 is shown in more detail in Fig. 10. The modeling results confirm that the PEM electrolyzer system can follow the variable wind power with a relatively high efficiency. The electrolyzer efficiency is in the range 72–88% and it is inversely correlated to the input power (higher input power gives relatively lower efficiency and vice versa). The average efficiency for a 31-day period is approximately 75%.

The explanation for why the efficiency changes inversely with the input power is found in the efficiency equation (equation (12)), which consists of the Faraday efficiency (equation (14)) and voltage efficiency (equation (13)). As seen in equation (14), the Faraday efficiency increases when the current i increases. Since power is directly correlated to current

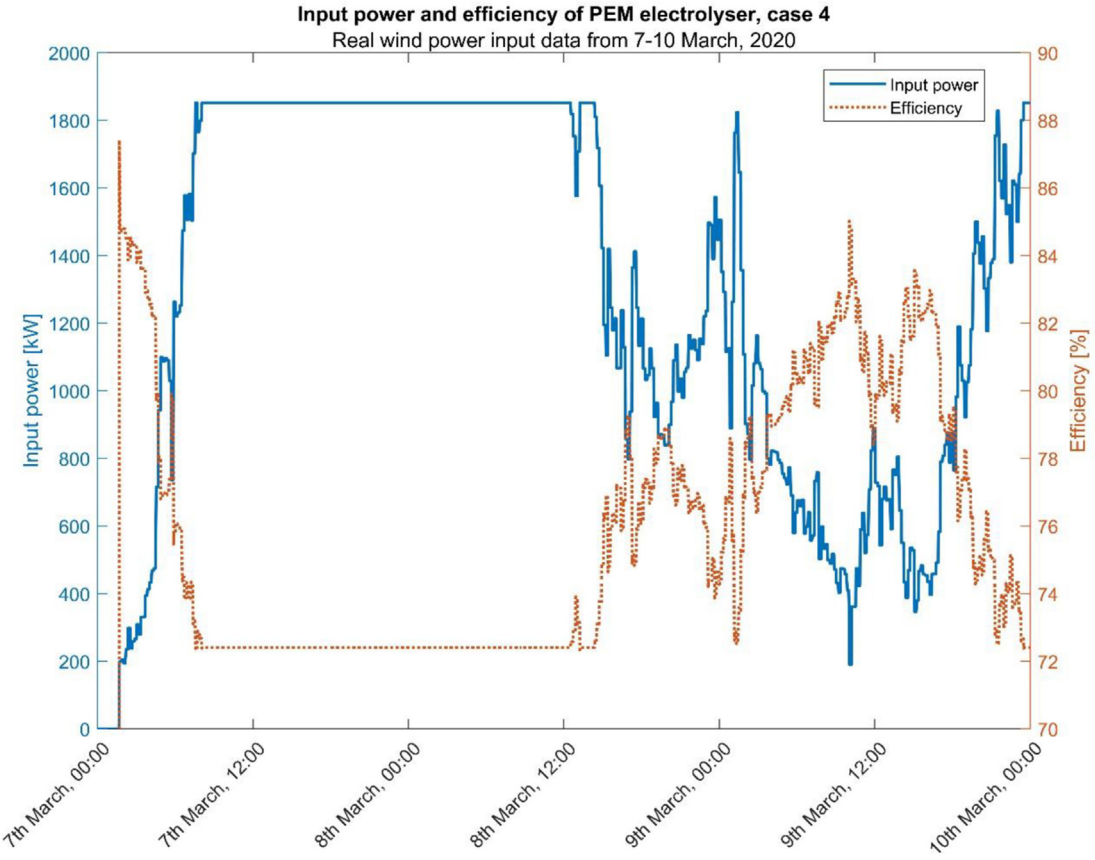

Fig. 10 – Efficiency and input power for the PEM electrolyzer in simulation case 4 during the 3-day period from 7th-10th March 2020. The electrolyzer operation is simulated using real wind power data from the given period as input.

(Power = voltage × current) the Faraday efficiency increases when the input power increases, and it stays in the range 92–99% (92% when the input power is at its minimum and 99% when the input power is at its maximum). However, as seen in equation (13) the voltage efficiency decreases when the input power increases, since the cell voltage is also directly correlated to power (Power = voltage × current). The range of the voltage efficiency is 72–95% (95% when the input power is at its minimum and 72% when the input power is at its maximum), which is a much wider range than the range of the Faraday efficiency. Therefore, the voltage efficiency has a larger effect on the total efficiency than the Faraday efficiency does. The total electrolyzer efficiency will therefore be at the lowest value when the input power is at its maximum, and at the highest value when the input power is at its minimum, as seen in Fig. 10.

Since the electrolyzer can follow the variations in wind power it is not beneficial to include a battery in the system. Most of the scenarios with batteries have higher production cost and slightly lower efficiency without increasing the hydrogen production, as shown in Table 4. However, again it should be noted that the advantage of including a battery in the system could prove to be higher in a real-world system where the wind power input to the electrolyzer will not be constant in each 10-min period, as it is in the simulations. This will be a subject for future experimental work.

Fig. 11 shows how the wind power is used during the same 3-day period of case 4. The electrolyzer uses most of the wind power. The compression and storage of hydrogen uses 7.4% of the total energy to the electrolyzer and storage system. For example, when the electrolyzer and storage system receives a total of 2000 kW of wind power, the electrolyzer uses 1852 kW and the storage system uses 148 kW. This can be seen in Fig. 11 in the period where the wind turbine is at maximum power (2300 kW). The onshore grid receives the excess wind power when the turbine produces more than 2000 kW. The grid also receives all the wind power when the wind turbine produces less than 200 kW (since the electrolyzer is set to shut down when the input power is less than 10% of the rated input power). This can be seen in the first minutes of Fig. 11. The energy for desalination of sea water is included in all simulations, but it is not shown in the figure since it is negligibly small compared to all the other energy usages. It is equal to approximately 0.1% of the energy used by the electrolyzer.

Fig. 12 shows the distribution of the wind energy in the 31-day period in case 4. In this case, 86% of the wind energy is used by the PEM electrolyzer, 7% is used to compress and store the hydrogen gas, and 7% goes to the onshore electricity grid. The desalination of sea water uses less than 1% of the total wind energy.

Fig. 13 shows the percentages of the total time in the 31-day period that the electrolyzer operated in each power interval. The intervals are defined in the following way: 1) **high power** if the input power to the electrolyzer is in the range 80–100% of its rated power, 2) **medium power** in the range 40–80% of rated

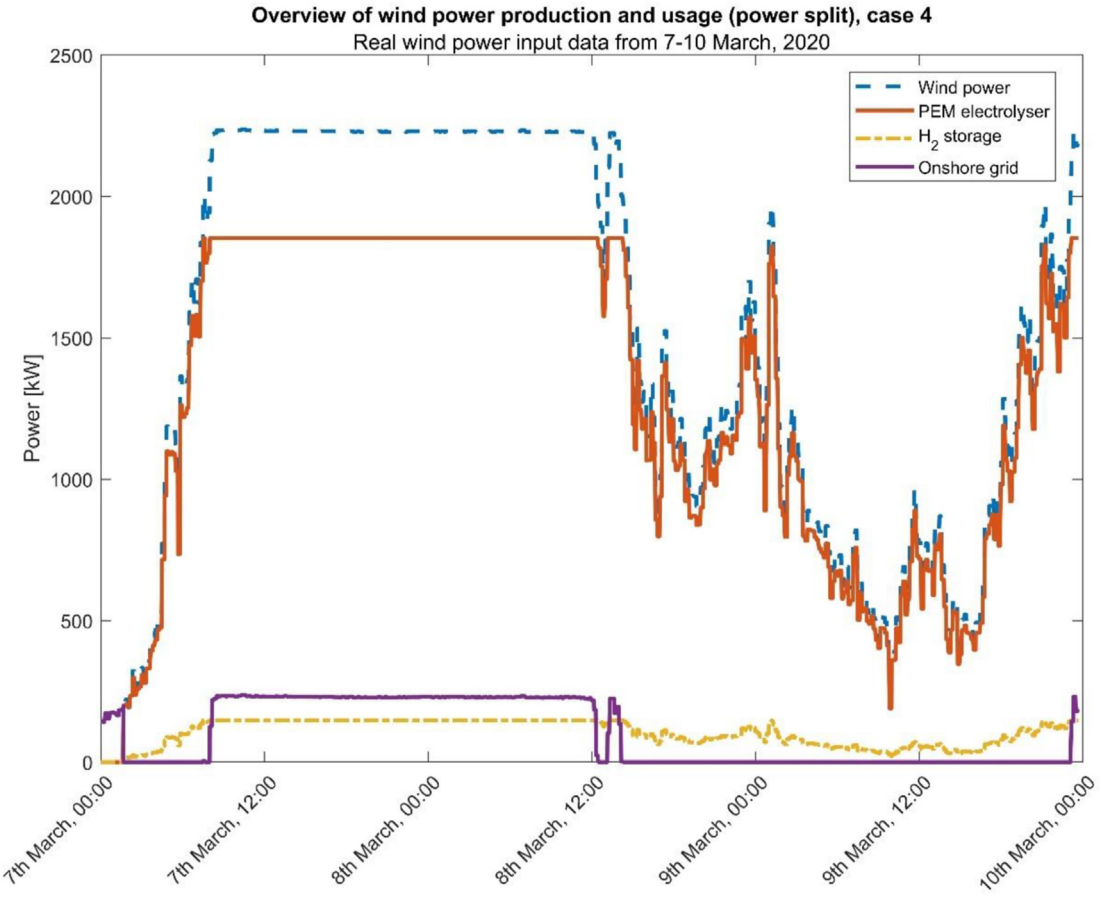

Fig. 11 – Overview of the wind power production and how it is used in simulation case 4 during a 3-day period from 7th-10th March 2020. The wind power production is real data input from the same period.

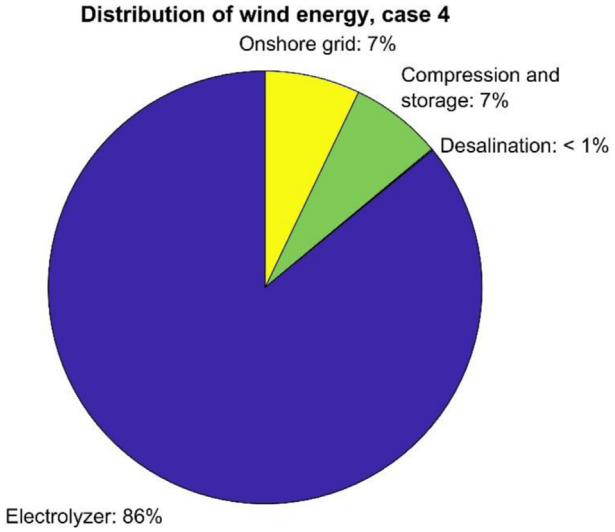

Fig. 12 – Distribution of wind energy in the period 7th March to April 6, 2020 for case 4.

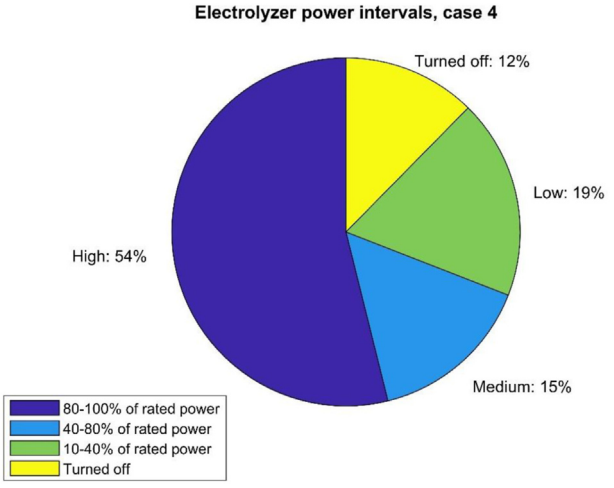

Fig. 13 – Percentage of total time in each power interval for the electrolyzer in case 4.

power, 3) **low power** in the range 10–40% of rated power. If the input power to the electrolyzer is below 10% of its rated power it will be turned off, as explained in Control system. During the 31-day period in case 4 the electrolyzer was switched off 43 times. Many of these were clustered quite closely together in periods were the wind power had large and rapid fluctuations. In case 1, which is identical to case 4 except that a lithium-ion battery is included in the system, the electrolyzer was only switched off 14 times in the same time period. This means that a 67% reduction in the number of shutdowns is achieved by

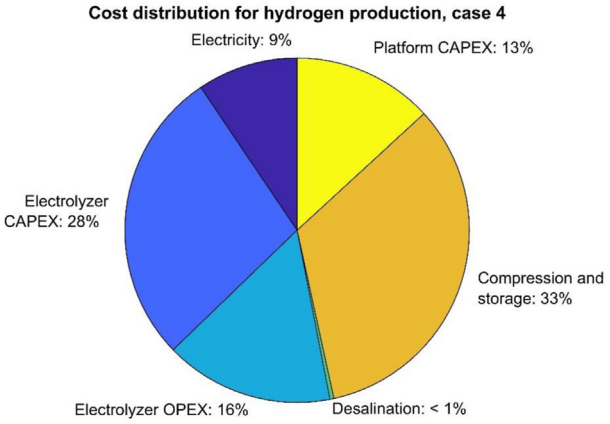

Fig. 14 – Cost distribution in percent for case 4.

including a battery. However, the reduced number of shutdowns did not impact the total hydrogen production or efficiency, as shown in Table 4. This should be tested in future experimental work, since the effect on hydrogen production and overall system efficiency by including a battery could prove to be greater in a real-world system.

Fig. 14 shows the cost distribution percentages in case 4. The electrolyzer costs are the highest with CAPEX (28%) and OPEX (16%) combined making up 44% of the total cost for this period. The cost of compressing and storing the hydrogen gas is also a big part of the total cost with 33%. The platform cost is 13% and the electricity cost is relatively low for this period at only 9% of the total cost. The cost of desalinating sea water is less than 1% of the total cost. The most important thing to note here is related to the electricity cost. The price of electricity in Norway during the 31-day period (7th March to April 6, 2020) used in case 4 was very low (see Table 2) and this cost was therefore a small part of the total cost. However, the electricity price has large fluctuations over time and has increased a lot since then. This is demonstrated very well by looking at case 16 which has an identical system design, but in this period (January 2022) the electricity price was almost 18 times higher (Table 2). This caused the electricity cost to be 62% of the total cost in case 16. The total cost for case 16 was 2.6 times higher than case 4, even though case 16 had a wind turbine capacity factor that was only slightly lower than it was in case 4. This indicates that the price of electricity could be the most important factor for the economic viability of these systems in the future.

Conclusions and future work

This study uses real-world energy production data measured on a 2.3 MW FOWT and Nord Pool electricity price data for the wind turbine's location as input to a detailed MATLAB/Simulink model that simulates offshore hydrogen production via a PEM water electrolyzer. Five different 31-day time periods are used in combination with six different wind/hydrogen-system designs, resulting in 30 unique system simulation cases. The three focus areas in this study are: (1) the total hydrogen production, (2) overall efficiency of the hydrogen production process, and (3) the hydrogen production cost.

The simulation results show how the total hydrogen production and production cost depend on both the wind turbine capacity factor and the price of electricity. The ideal conditions for an offshore hydrogen production system of this type are a high wind turbine capacity factor combined with a low electricity price. The difference between a "good" and a "bad" month can be as high as a factor of three for both the total hydrogen production and hydrogen production cost. As expected, this implies that the profitability of a system of this type will vary greatly from month to month.

The lowest hydrogen production costs are, as expected, achieved in the time period with the most favorable conditions, and are in the range 4.53–5.46 $/kg H_2. The highest total hydrogen production achieved during a 31-day period was 17 242 kg using a 1852 kW electrolyzer (i.e., an electrolyzer utilization factor of ca. 68%). The overall efficiency of the process was very similar for all the different simulation cases due to the load-following capabilities in the modeling of the PEM water electrolyzer system. The overall efficiency was in the range 56.1–56.9% (LHV) for all the cases.

The results also indicate that it is not favorable to include a battery in the system since this increases the hydrogen production cost without increasing the total hydrogen production. However, this will need to be verified in a real-world system that is not subject to the limitations and simplifications used in these simulations. There are several areas of future work that should be performed to expand and validate the results of this study, including.

- Develop a more detailed economical model that includes the time value of money (discount rate).
- Expand the MATLAB/Simulink model to include:
  - -Power electronics
  - -Ramp-up and start-up times and rates for the electrolyzer (i.e., typical changes in power input to the electrolyzer from one time step to the next. For example, 10% change in power x % of the time, 20% change in power y % of the time, etc.)
  - -Energy usage by the electrolyzer when it is in standby mode
  - -Dynamic models of the hydrogen storage system (e.g., hydrogen compressor) and desalination system instead of using constants from literature
- Build and test a real-world pilot system to validate the simulation results.

Declaration of competing interest

The authors declare that they have no known competing financial interests or personal relationships that could have appeared to influence the work reported in this paper.

Acknowledgements

The authors would like to acknowledge the Research Council of Norway for partly funding the work in this study (project number 295605).

Appendix A. Supplementary data

Supplementary data to this article can be found online at https://doi.org/10.1016/j.ijhydene.2023.03.471.

REFERENCES

[1] Deep Purple™ pilot - TechnipFMC plc. https://www.technipfmc.com/en/what-we-do/new-energy-ventures/hydrogen/deep-purple-pilot/. [Accessed 6 July 2022].
[2] Green hydrogen. https://www.siemensgamesa.com/en-int/products-and-services/hybrid-and-storage/green-hydrogen. [Accessed 6 July 2022].
[3] PosHYdon pilot Dutch North Sea | Neptune energy. https://www.neptuneenergy.com/esg/poshydon-hydrogen-pilot. [Accessed 6 July 2022].
[4] Erm Dolphyn. https://ermdolphyn.erm.com/p/1. [Accessed 6 July 2022].
[5] Meier K. Hydrogen production with sea water electrolysis using Norwegian offshore wind energy potentials. Int. J Energy Environ. Eng Times 2014;5:104. https://doi.org/10.1007/s40095-014-0104-6.
[6] Loisel R, Baranger L, Chemouri N, Spinu S, Pardo S. Economic evaluation of hybrid off-shore wind power and hydrogen storage system. Int J Hydrogen Energy 2015;40(21):6727–39. https://doi.org/10.1016/j.ijhydene.2015.03.117.
[7] Schnuelle C, Wassermann T, Fuhrlaender D, Zondervan E. Dynamic hydrogen production from PV and wind direct electricity supply – modeling and techno-economic assessment. Int J Hydrogen Energy 2020;45(55):29938–52. https://doi.org/10.1016/j.ijhydene.2020.08.044.
[8] McDonagh S, Ahmed S, Desmond C, Murphy JD. Hydrogen from offshore wind: investor perspective on the profitability of a hybrid system including for curtailment. Appl. Energy 2020;265:114732. https://doi.org/10.1016/j.apenergy.2020.114732.
[9] Dinh VN, Leahy P, McKeogh E, Murphy J, Cummins V. Development of a viability assessment model for hydrogen production from dedicated offshore wind farms. Int J Hydrogen Energy 2021;46(48):24620–31. https://doi.org/10.1016/j.ijhydene.2020.04.232.
[10] Calado G, Castro R. Hydrogen production from offshore wind parks: current situation and future perspectives. Appl Sci 2021;11(12):5561. https://doi.org/10.3390/app11125561.
[11] Song S, et al. Production of hydrogen from offshore wind in China and cost-competitive supply to Japan. Nat Commun Now 2021;12(no. 6953). https://doi.org/10.1038/s41467-021-27214-7.
[12] Ibrahim OS, Singlitico A, Proskovics R, McDonagh S, Desmond C, Murphy JD. Dedicated large-scale floating offshore wind to hydrogen: assessing design variables in proposed typologies. Renew Sustain Energy Rev 2022;160:112310. https://doi.org/10.1016/j.rser.2022.112310.
[13] J. Settino, R. N. Farrugia, D. Buhagiar, and T. Sant, Offshore wind-to-hydrogen production plant integrated with an innovative hydro-pneumatic energy storage device J Phys Conf Ser, vol. 2151, no. 12013, doi: 10.1088/1742-6596/2151/1/012013.
[14] Scolaro M, Kittner N. Optimizing hybrid offshore wind farms for cost-competitive hydrogen production in Germany. Int J Hydrog Energy 2022;47(10):6478–93. https://doi.org/10.1016/j.ijhydene.2021.12.062.
[15] Lucas TR, Ferreira AF, Santos Pereira RB, Alves M. Hydrogen production from the WindFloat Atlantic offshore wind farm: a techno-economic analysis. Appl Energy 2022;310:118481. https://doi.org/10.1016/j.apenergy.2021.118481.
[16] Tebibel H. Methodology for multi-objective optimization of wind turbine/battery/electrolyzer system for decentralized clean hydrogen production using an adapted power management strategy for low wind speed conditions. Energy Convers Manag Jun. 2021;238:114125. https://doi.org/10.1016/j.enconman.2021.114125.
[17] Jang D, Kim K, Kim K-H, Kang S. Techno-economic analysis and Monte Carlo simulation for green hydrogen production using offshore wind power plant. Energy Convers Manag Jul. 2022;263:115695. https://doi-org.ezproxy.uio.no/10.1016/j.enconman.2022.115695.
[18] Luo Z, Wang X, Wen H, Pei A. Hydrogen production from offshore wind power in South China. Int J Hydrogen Energy Jul. 2022;47(58):24558–68. https://doi-org.ezproxy.uio.no/10.1016/j.ijhydene.2022.03.162.
[19] Baldi F, et al. Optimisation-based system designs for deep offshore wind farms including power to gas technologies. Appl Energy Mar. 2022;310:118540. https://doi-org.ezproxy.uio.no/10.1016/j.apenergy.2022.118540.
[20] Benalcazar P, Komorowska A. Prospects of green hydrogen in Poland: a techno-economic analysis using a Monte Carlo approach. Int J Hydrogen Energy Jan. 2022;47(9):5779–96. https://doi-org.ezproxy.uio.no/10.1016/j.ijhydene.2021.12.001.
[21] Lamagna M, Monforti Ferrario A, Astiaso Garcia D, Mcphail S, Comodi G. Reversible solid oxide cell coupled to an offshore wind turbine as a poly-generation energy system for auxiliary backup generation and hydrogen production. Energy Rep Nov. 2022;8:14259–73. https://doi.org/10.1016/j.egyr.2022.10.355.
[22] Nasser M, Megahed TF, Ookawara S, Hassan H. Techno-economic assessment of clean hydrogen production and storage using hybrid renewable energy system of PV/Wind under different climatic conditions. Sustain Energy Technol Assess Aug. 2022;52(B):102195. https://doi.org/10.1016/j.seta.2022.102195.
[23] Corengia M, Torres AI. Coupling time varying power sources to production of green-hydrogen: a superstructure based approach for technology selection and optimal design. Chem Eng Res des 2022;183:235–49. https://doi.org/10.1016/j.cherd.2022.05.007.
[24] Groenemans H, Saur G, Mittelsteadt C, Lattimer J, Xu H. Techno-economic analysis of offshore wind PEM water electrolysis for H_2 production. Current Opinion in Chem Engin 2022;37:100828. https://doi.org/10.1016/j.coche.2022.100828.
[25] Dinh QV, Dinh VN, Mosadeghi H, Pereira PHT, Leahy PG. A geospatial method for estimating the levelized cost of hydrogen production from offshore wind. Int J Hydrogen Energy 2023. https://doi.org/10.1016/j.ijhydene.2023.01.016.
[26] Komorowska A, Benalcazar P, Kaminski J. Evaluating the competitiveness and uncertainty of offshore wind-to-hydrogen production: a case study of Poland. Int J Hydrogen Energy 2023;48:14577–90. https://doi.org/10.1016/j.ijhydene.2023.01.015.
[27] Kim A, Kim H, Choe C, Lim H. Feasibility of offshore wind turbines for linkage with onshore green hydrogen demands: a comparative economic analysis. Energy Convers Manag 2023;277:116662. https://doi.org/10.1016/j.enconman.2023.116662.
[28] Gea-Bermúdez J, Bramstoft R, Koivisto M, Kitzing L, Ramos A. Going offshore or not: where to generate hydrogen in future integrated energy systems? Energy Pol 2023;174:113382. https://doi.org/10.1016/j.enpol.2022.113382.

[29] Durakovic G, del Granado PC, Tomasgard A. Powering Europe with North Sea offshore wind: the impact of hydrogen investments on grid infrastructure and power prices. Energy 2023;263:125654. https://doi.org/10.1016/j.energy.2022.125654.
[30] Backe S, Skar C, del Granado PC, Turgut O, Tomasgard A. EMPIRE: an open-source model based on multi-horizon programming for energy transition analyses. SoftwareX 2022;17:100877. https://doi.org/10.1016/j.softx.2021.100877.
[31] Kumar S, Baalisampang T, Arzaghi E, Garaniya V, Abbassi R, Salehi F. Synergy of green hydrogen sector with offshore industries: opportunities and challenges for a safe and sustainable hydrogen economy. J Clean Prod 2023;384:135545. https://doi.org/10.1016/j.jclepro.2022.135545.
[32] Li R, et al. Techno-economic analysis of a wind-photovoltaic-electrolysis-battery hybrid energy system for power and hydrogen generation. Energy Convers Manag 2023;281:116854. https://doi.org/10.1016/j.enconman.2023.116854.
[33] Giampieri A, Ling-Chin J, Roskilly AP. Techno-economic assessment of offshore wind-to-hydrogen scenarios: a UK case study. Int J Hydrogen Energy 2023. https://doi.org/10.1016/j.ijhydene.2023.01.346.
[34] Nasser M, Hassan H. Techno-enviro-economic analysis of hydrogen production via low and high temperature electrolyzers powered by PV/Wind turbines/Waste heat. Energy Convers Manag 2023;278:116693. https://doi.org/10.1016/j.enconman.2023.116693.
[35] Cheng C, Hughes L. The role for offshore wind power in renewable hydrogen production in Australia. J Clean Prod 2023;391:136223. https://doi.org/10.1016/j.jclepro.2023.136223.
[36] Simulink - Simulation and Model-Based Design - Matlab & Simulink. https://se.mathworks.com/products/simulink.html. [Accessed 5 July 2022].
[37] Umbilical & Flying Leads - Unitech Energy GroupUnitech Energy Group. https://unitechenergy.com/. [Accessed 5 July 2022].
[38] Market data | Nord Pool. https://www.nordpoolgroup.com/en/market-data-for-media/. [Accessed 20 December 2022].
[39] Jensen JF. Proton exchange membrane water electrolyzer modeling, master's thesis. Oslo: University of Oslo; 2021.
[40] Hancke R, Holm T, Ø Ulleberg. The case for high-pressure PEM water electrolysis. Energy Convers Manag Apr. 2022;261:115642. https://doi.org/10.1016/j.enconman.2022.115642.
[41] Hancke R, Piotr B, Holm T, Ø Ulleberg. In: Performance of high-pressure PEM water electrolysis system, presented at the International Conference on Electrolysis, Golden, Colorado, USA; Jun. 2022.
[42] Arkivbilder – bilder, vektorer og illustrasjoner for kreative prosjekter | Shutterstock. https://www.shutterstock.com/nb. [Accessed 6 July 2022].
[43] Buttler A, Spliethoff H. Current status of water electrolysis for energy storage, grid balancing and sector coupling via power-to-gas and power-to-liquids: a review. Renew Sustain Energy Rev 2018;82(3):2440–54. https://doi.org/10.1016/j.rser.2017.09.003.
[44] Sæbø AO, et al. Optimal utnyttelse av energi fra havvind i Sørlige Nordsjø II, Greenstat, Æge Energy, University of Bergen, Western Norway University of Applied Sciences, Technical report. Apr. 2021.
[45] M Series Containerized Pem Electrolysers | Nel Hydrogen. https://nelhydrogen.com/resources/m-series-containerized-pem-electrolysers/. [Accessed 5 July 2022].
[46] Lithium Ion – Lithium Ion Battery Test Centre. https://batterytestcentre.com.au/project/lithium-ion/. [Accessed 5 July 2022].
[47] Mongird K, et al. Energy storage technology and cost characterization report, US department of energy. Technical report Jul. 2019.
[48] Parks G, Boyd R, Cornish J, Remick R. Hydrogen station compression, storage, and dispensing - technical status and costs, National renewable energy laboratory. Technical report May 2014.
[49] The Future of Hydrogen,International energy Agency. Technical report Jun. 2019.
[50] Schalenbach M, Carmo M, Fritz DL, Mergel J, Stolten D. Pressurized PEM water electrolysis: efficiency and gas crossover. Int J Hydrogen Energy 2013;38(35):14921–33. https://doi.org/10.1016/j.ijhydene.2013.09.013.
[51] Liso V, Savoia G, Araya SS, Cinti G, Kær SK. Modeling and experimental analysis of a polymer electrolyte membrane water electrolysis cell at different operating temperatures. Energies 2018;11(12):3273. https://doi.org/10.3390/en11123273.
[52] Abdin Z, Webb CJ, MacA E. Gray, Modeling and simulation of a proton exchange membrane (PEM) electrolyser cell. Int J Hydrogen Energy 2015;40(39):13243–57. https://doi.org/10.1016/j.ijhydene.2015.07.129.
[53] Coutanceau C, Baranton S, Audichon T. Chapter 3-hydrogen production from water electrolysis, in. Hyd Electrochem Prod 2018:17–62.
[54] Carmo M, Stolten D. Chapter 4-energy storage using hydrogen produced from excess renewable electricity: power to hydrogen, in *Science and Engineering of hydrogen-based energy technologies*. Academic Press; 2019. p. 165–99.
[55] Garcìa-Valverde R, Espinosa N, Urbina A. Simple PEM water electrolyser model and experimental validation. Int J Hydrogen Energy 2012;37(2):1927–38. https://doi.org/10.1016/j.ijhydene.2011.09.027.
[56] Carmo M, Fritz DL, Mergel J, Stolten D. A comprehensive review on PEM water electrolysis. Int J Hydrogen Energy 2013;38(12):4901–34. https://doi.org/10.1016/j.ijhydene.2013.01.151.
[57] Tiktak J. Heat management of PEM electrolysis, master's thesis. Delft: Delft University of Technology; 2019 [Online]. Available, https://repository.tudelft.nl/islandora/object/uuid:c046820a-72bc-4f05-b72d-e60a3ecb8c89?collection=education.
[58] Dale NV, Mann MD, Salehfar H. Semiempirical model based on thermodynamic principles for determining 6 kW proton exchange membrane electrolyzer stack characteristics. J Power Sources 2008;185(2):1348–53. https://doi.org/10.1016/j.jpowsour.2008.08.054.
[59] Harrison KW, Remick R, Martin GD, Hoskin A. Hydrogen production: fundamentals and case study summaries, national renewable energy laboratory. Technical report Jan. 2010 [Online]. Available, https://www.nrel.gov/docs/fy10osti/47302.pdf.
[60] Scheepers F, et al. Improving the efficiency of PEM electrolyzers through membrane-specific pressure optimization. Energies 2020;13(3):612. https://doi.org/10.3390/en13030612.
[61] Hydrogen | Properties, Uses, & Facts | Britannica. https://www.britannica.com/science/hydrogen. [Accessed 5 July 2022].
[62] Hydrogen Economy Outlook, Bloomberg new energy finance. Technical report Mar. 2020.
[63] Gielen D, Taibi E, Miranda R. Hydrogen: a renewable energy perspective, International renewable energy Agency. Technical report Sep. 2019 [Online]. Available, https://www.

irena.org/publications/2019/Sep/Hydrogen-A-renewable-energy-perspective.

[64] Mahone A, et al. Hydrogen opportunities in a low-carbon future, Energy+Environmental economics. Technical report Jun. 2020 [Online]. Available, https://www.ethree.com/wp-content/uploads/2020/07/E3_MHPS_Hydrogen-in-the-West-Report_Final_June2020.pdf.

[65] Path to hydrogen competitiveness - A cost perspective, hydrogen Council. Technical report Jan. 2020 [Online]. Available, https://hydrogencouncil.com/wp-content/uploads/2020/01/Path-to-Hydrogen-Competitiveness_Full-Study-1.pdf.

[66] Vickers J, Peterson D, Randolph K. Cost of electrolytic hydrogen production with existing technology, US department of energy. Technical report Sep. 2020;20004 [Online]. Available, https://www.hydrogen.energy.gov/pdfs/20004-cost-electrolytic-hydrogen-production.pdf.

[67] Energy density. Wikipedia Jun. 15, 2022 [Online]. Available, https://en.wikipedia.org/w/index.php?title=Energy_density&oldid=1093209331. [Accessed 5 July 2022].